PFC/JA-86-34

SINGLE-PARTICLE ANALYSIS OF THE FREE ELECTRON LASER SIDEBAND INSTABILITY FOR PRIMARY ELECTROMAGNETIC WAVE WITH CONSTANT PHASE AND SLOWLY VARYING PHASE

Ronald C. Davidson
and
Jonathan S. Wurtele

June, 1986

Plasma Fusion Center
Massachusetts Institute of Technology
Cambridge, Massachusetts 02139 USA

This research was supported in part by the Los Alamos National Laboratory and in part by the Office of Naval Research.

Submitted for publication in Physics of Fluids.

SINGLE-PARTICLE ANALYSIS OF THE FREE ELECTRON LASER SIDEBAND INSTABILITY FOR PRIMARY ELECTROMAGNETIC WAVE WITH CONSTANT PHASE AND SLOWLY VARYING PHASE

Ronald C. Davidson*
Science Applications International Corporation, Boulder, Colorado 80302

Jonathan S. Wurtele
Plasma Fusion Center
Massachusetts Institute of Technology, Cambridge, Massachusetts 02139

ABSTRACT

Use is made of the single-particle orbit equations together with Maxwell's equations and appropriate statistical averages to investigate detailed properties of the sideband instability for a helical-wiggler free electron laser with wiggler wavelength $\lambda_0 = 2\pi/k_0 = \text{const.}$ and normalized wiggler amplitude $a_w = e\hat{B}_w/mc^2k_0 = \text{const.}$ The model describes the nonlinear evolution of a right-circularly-polarized primary electromagnetic wave with frequency ω_s, wavenumber k_s, and slowly varying amplitude $\hat{a}_s(z,t)$ and phase $\delta_s(z,t)$ (Eikonal approximation). The orbit and wave equations are analysed in the ponderomotive frame ("primed" variables) moving with velocity $v_p = \omega_s/(k_s + k_0)$ relative to the laboratory. Detailed properties of the sideband instability are investigated for small-amplitude perturbations about a quasi-steady equilibrium state characterized by $\hat{a}_s^0 = \text{const.}$ (independent of z' and t'). Two cases are treated. The first case assumes constant equilibrium wave phase $\delta_s^0 = \text{const.}$, which requires (for self-consistency) both untrapped- and trapped-electron populations satisfying $\left\langle \sum_j \exp[ik_p' z_{j0}'(t') + i\delta_s^0]/\gamma_j' \right\rangle = 0$. Here, $k_p' = (k_s + k_0)/\gamma_p$ is the wavenumber of the ponderomotive potential; $z_{j0}'(t')$ is the equilibrium orbit; and $\gamma_j' mc^2$ is the electron energy. The second case assumes that all of the electrons are deeply trapped, which requires a slow spatial variation of the equilibrium wave phase, $\partial\delta_s^0/\partial z' = 2\Gamma_0(\Gamma_0 ck_0/\Omega_B)^2 k_p' \neq 0$. The resulting dispersion relations and detailed stability properties are found to be quite different in the two cases. Both the weak-pump and strong-pump regimes are considered.

---

* Permanent address: Plasma Fusion Center, Massachusetts Institute of Technology, Cambridge, MA 02139

I. INTRODUCTION AND SUMMARY

There is growing experimental[1-18] and theoretical[19-65] interest in free electron lasers (FELs)[66-69] as effective sources for coherent radiation generation by intense relativistic electron beams. Recent theoretical studies have included investigations of nonlinear effects[19-42] and saturation mechanisms, the influence of finite geometry on linear stability properties,[43-48] novel magnetic field geometries for radiation generation,[43,49-53] and fundamental studies of stability behavior.[54-65] One topic of considerable practical interest is the sideband instability[32] which results from the bounce motion of electrons trapped in the (finite-amplitude) ponderomotive potential. Both kinetic[19-21] and single-particle[32-42] models of the sideband instability have been developed, and numerical simulations[34-42] have been carried out. However, with the exception of the recent kinetic studies by Davidson et.al.,[19-21] the theoretical models have assumed perturbations about a finite-amplitude primary electromagnetic wave with slowly varying equilibrium phase δ_s^0. By including both untrapped- and trapped-electron populations, it has been shown[21] that quasi-steady equilibrium solutions to the nonlinear Vlasov-Maxwell equations exist in which both the amplitude and phase of the primary electromagnetic wave are constant. Moreover, the concomitant kinetic investigations[19,20] of the sideband instability for δ_s^0 = const. have shown that linear stability properties are qualitatively and quantitatively different from single-particle treatments[32-42] of the sideband instability carried out for the case where the equilibrium wave phase δ_s^0 is slowly varying. In the present analysis, we use a single model to investigate detailed linear properties of the sideband instability for both cases (constant wave phase, and slowly varying

phase). The theoretical model (Secs. II-IV) is based on the single-particle orbit equations together with Maxwell's equations and appropriate statistical averages.[32] Unlike earlier single-particle treatments, the present analysis is carried out in the ponderomotive frame, which leads to a considerable simplification in the orbit equations.

The theoretical model and assumptions are described in Secs. II-IV. A tenuous, relativistic electron beam propagates through a constant-amplitude helical wiggler magnetic field with wavelength $\lambda_0 = 2\pi/k_0 = \text{const.}$, normalized amplitude $a_w = e\hat{B}_w/mc^2k_0 = \text{const.}$, and vector potential specified by [Eq.(1)]

$$\underset{\sim}{A}_w(\underset{\sim}{x}) = -\frac{mc^2}{e}\, a_w\left(\cos k_0 z\hat{\underset{\sim}{e}}_x + \sin k_0 z\hat{\underset{\sim}{e}}_y\right) .$$

The model neglects longitudinal perturbations (Compton-regime approximation with $\delta\phi \simeq 0$) and transverse spatial variations ($\partial/\partial x = 0 = \partial/\partial y$). Moreover, the analysis is carried out for the case of a finite-amplitude primary electromagnetic wave (ω_s, k_s) with right-circular polarization and vector potential specified by [Eq.(2)]

$$\underset{\sim}{A}_s(\underset{\sim}{x},t) = \frac{mc^2}{e}\,\hat{a}_s(z,t)\left\{\cos[k_s z - \omega_s t + \delta_s(z,t)]\hat{\underset{\sim}{e}}_x\right.$$

$$\left. - \sin[k_s z - \omega_s t + \delta_s(z,t)]\hat{\underset{\sim}{e}}_y\right\} ,$$

where the normalized amplitude $\hat{a}_s(z,t)$ and wave phase $\delta_s(z,t)$ are treated as slowly varying (Eikonal approximation). A detailed investigation of the sideband instability simplifies considerably if the analysis is carried out in the ponderomotive frame moving with velocity [Eq.(3)][19-21]

$$v_p = \frac{\omega_s}{k_s + k_0} .$$

In the ponderomotive frame ("primed" variables), the nonlinear evolution of $\hat{a}_s(z',t')$ and $\delta_s'(z',t')$ is described by [Eqs.(24) and (25)]

$$2\omega_s'\left(\frac{\partial}{\partial t'} + \frac{k_s'c^2}{\omega_s'}\frac{\partial}{\partial z'}\right)\hat{a}_s = \frac{4\pi e^2 a_w}{m}\frac{1}{L'}\left\langle \sum_j \frac{\sin(\theta_{js}' + \delta_s')}{\gamma_j'} \right\rangle ,$$

$$2\omega_s'\hat{a}_s\left(\frac{\partial}{\partial t'} + \frac{k_s'c^2}{\omega_s'}\frac{\partial}{\partial z'}\right)\delta_s' = \frac{4\pi e^2 a_w}{m}\frac{1}{L'}\left\langle \sum_j \frac{\cos(\theta_{js}' + \delta_s')}{\gamma_j'} \right\rangle ,$$

where the statistical average $L'^{-1}\left\langle \sum_j \cdots \right\rangle$ is defined in Eq.(27). Here, correct to lowest order in $|(\omega_s'/\hat{a}_s)(\partial \hat{a}_s/\partial t')|<<1$, energy is conserved in the ponderomotive frame ($d\gamma_j'/dt' = 0$), and the axial orbit $\theta_{js}'(t') = k_p' z_j'(t')$ solves [Eq.(35)]

$$\frac{d^2}{dt'^2}\theta_{js}' + \frac{c^2 k_p'^2 a_w}{\gamma_j'^2}\,\mathrm{Im}\left[\hat{a}_s \exp(i\theta_{js}' + i\delta_s')\right] = 0 ,$$

where $k_p' = (k_s + k_0)/\gamma_p$ is the wavenumber of the ponderomotive potential. Moreover, the real oscillation frequency ω_s' and wavenumber k_s' are related by the dispersion relation [Eq.(20)].

$$\omega_s'^2 = c^2 k_s'^2 + \frac{4\pi e^2}{m}\frac{1}{L'}\left\langle \sum_j \frac{1}{\gamma_j'} \right\rangle .$$

In obtaining Eqs.(20), (24), (25) and (35), it is assumed that all electrons have zero transverse canonical momentum, i.e., $P_{xj}' = 0 = P_{yj}'$.

Equations (24), (25) and (35) are used to investigate properties of the sideband instability for small-amplitude perturbations about a primary

electromagnetic wave with constant amplitude $\hat{a}_s^0$ = const. (independent of z' and t'). Two cases are treated. The first case (Sec.V) assumes constant equilibrium wave phase δ_s^0 = const., which requires (for self-consistency) both untrapped- and trapped-electron populations satisfying $\langle \sum_j \gamma_j'^{-1} \exp(i\theta_{js}^0 + i\delta_s^0) \rangle = 0$ [Eq.(49)]. This is analogous to the case studied by Davidson et. al.[19-21] using the Vlasov-Maxwell equations. The second case (Sec. VI) assumes that all of the electrons are trapped, which requires a slow spatial variation of the equilibrium wave phase $\partial\delta_s^0/\partial z' \neq 0$.[32-42] The resulting dispersion relations and detailed stability properties are found to be quite different in the two cases. For deeply trapped electrons, it is shown that the two dispersion relations are given by [Eq.(68)]

$$(\Delta\Omega - c\Delta K)\left[(\Delta\Omega)^2 - \Omega_B^2\right] = \Gamma_0^3 c^3 k_0^3$$

for δ_s^0 = const. (Sec. V), and by [Eq.(94)]

$$0 = 1 - \frac{\Omega_B^2}{(\Delta\Omega)^2} - \frac{\Omega_B^2 4(\Gamma_0 c k_0/\Omega_B)^6}{(\Delta\Omega - c\Delta K)^2}$$

for $\partial\delta_s^0/\partial z' = 2\Gamma_0(\Gamma_0 c k_0/\Omega_B)^2 k_p' \neq 0$ (Sec. VI). In Eqs.(68) and (94), $\Delta\Omega$ and ΔK are defined by $\Delta\Omega = \Delta\omega - v_p\Delta k$ and $\Delta K = k_0(v_p/c)\Delta k/k_s$, where we have transformed back to the laboratory-frame frequency $\omega = \omega_s + \Delta\omega$ and wave-number $k = k_s + \Delta k$. Moreover, the small parameter Γ_0^3 is defined by [Eq.(39)]

$$\Gamma_0^3 = \frac{1}{4}\frac{a_w^2}{\hat{\gamma}'^3}\frac{\hat{\omega}_{pT}^2}{\gamma_p^2 c^2 k_0^2}\frac{(1 + v_p/c)}{v_p/c} << 1 ,$$

and Ω_B is the bounce frequency in the laboratory frame

$$\Omega_B = \left(\frac{c^2 k_p'^2 a_w \hat{a}_s^0}{\hat{\gamma}'^2 \gamma_p^2} \right)^{1/2} .$$

Here, γ_p is defined by $\gamma_p = (1 - v_p^2/c^2)^{1/2}$, $\hat{\gamma}' \simeq (1 + a_w^2)^{1/2}$ is the characteristic energy of the trapped electrons, and $\hat{\omega}_{pT}^2 = 4\pi \hat{n}_T' e^2/m = 4\pi \hat{n}_T e^2/\gamma_p m$ is the plasma frequency-squared of the trapped electrons.

The dispersion relations for $\delta_s^0 = $ const. [Eq.(68)] and $\partial \delta_s^0/\delta z' \neq 0$ [Eq.(94)] and the corresponding properties of the sideband instability are examined in detail in Secs. V and VI. We summarize here some of the key results.

(a) In the weak-pump regime ($\Omega_B/\Gamma_0 c k_0 << 1$), the characteristic maximum growth rate of the sideband instability is substantial, with $\mathrm{Im}(\Delta\Omega)_M/\Gamma_0 c k_0 = (3)^{1/2}/2$ in both cases [Eqs.(73) and (100)].

(b) In the strong-pump regime ($\Omega_B/\Gamma_0 c k_0 >> 1$), however, the maximum growth rate is reduced significantly, with $\mathrm{Im}(\Delta\Omega)_M/\Gamma_0 c k_0 = 2^{-1/2}(\Gamma_0 c k_0/\Omega_B)^{1/2} << 1$ for the case of constant phase δ_s^0 [Eq.(68)], and $\mathrm{Im}(\Delta\Omega)_M/\Gamma_0 c k_0 = \left[(3)^{1/2}/(2)^{2/3}\right](\Gamma_0 c k_0/\Omega_B) << 1$ for the case of slowly varying δ_s^0 [Eq.(94)].

(c) The instability bandwidth ΔK_b in ΔK-space is generally different in the two cases. For example, in the strong-pump regime ($\Omega_B/\Gamma_0 c k_0 >> 1$), it is found that $\Delta K_b/\Gamma_0 k_0 = (2\Gamma_0 c k_0/\Omega_B)^{1/2} << 1$ from Eq.(68), whereas $\Delta K_b/\Gamma_0 k_0 = \Omega_B/\Gamma_0 c k_0 >> 1$ follows from Eq.(94).

(d) Finally, for the case of slowly varying phase δ_s^0 [Eq.(94)], it is found that both the upper and lower sidebands are unstable, with $\mathrm{Re}(\Delta\Omega) > 0$ for $\Delta K > 0$ and $\mathrm{Re}(\Delta\Omega) < 0$ for $\Delta K < 0$. In contrast, for $\delta_s^0 = $ const., it is found from Eq.(68) that only the lower sideband is unstable. This is associated with the fact that the wave perturbation is assumed to have

right-circular polarization in deriving Eq.(68).[19] For δ_s^0 = const. and wave perturbations with left-circular polarization, it is readily shown that the upper sideband is unstable.[19]

II. THEORETICAL MODEL AND FIELD EQUATIONS

The present analysis assumes a tenuous, relativistic electron beam propagating in the z-direction through a helical magnetic wiggler field with vector potential

$$\begin{aligned} \underset{\sim}{A}_w(\underset{\sim}{x}) &= \frac{mc^2}{e}\,\underset{\sim}{a}_w(\underset{\sim}{x}) \\ &= -\frac{mc^2}{e}\,a_w(\cos k_0 z\,\hat{\underset{\sim}{e}}_x + \sin k_0 z\,\hat{\underset{\sim}{e}}_y)\ . \end{aligned} \tag{1}$$

Here, $-e$ is the electron charge, mc^2 is the electron rest energy, $\lambda_0 = 2\pi/k_0$ = const. is the wiggler wavelength, the wiggler magnetic field is $\underset{\sim}{B}_w = \nabla \times \underset{\sim}{A}_w$, and $a_w = e\hat{B}_w/mc^2k_0$ is the normalized wiggler amplitude. Transverse spatial variations are neglected ($\partial/\partial x = 0 = \partial/\partial y$), and it is assumed that the beam density and current are sufficiently low that the equilibrium self fields associated with the space charge and axial current of the electron beam are negligibly small. Moreover, longitudinal perturbations are neglected in the stability analysis (Compton-regime approximation with $\delta\phi \simeq 0$). In addition to the static wiggler field in Eq.(1), it is assumed that a primary electromagnetic wave signal with right-circular polarization has developed with vector potential

$$\begin{aligned} A_s(\underset{\sim}{x},t) &= \frac{mc^2}{e}\,\underset{\sim}{a}_s(\underset{\sim}{x},t) \\ &= \frac{mc^2}{e}\,\hat{a}_s(z,t)\Big\{\cos[k_s z - \omega_s t + \delta_s(z,t)]\hat{\underset{\sim}{e}}_x \\ &\qquad - \sin[k_s z - \omega_s t + \delta_s(z,t)]\hat{\underset{\sim}{e}}_y\Big\}\ , \end{aligned} \tag{2}$$

where ω_s and k_s are the frequency and wavenumber, respectively. Here, the wave amplitude $\hat{a}_s(z,t)$ and phase shift $\delta_s(z,t)$ are treated as slowly varying,

and the corresponding electromagnetic fields are given by $\underset{\sim}{B}_s = \nabla \times \underset{\sim}{A}_s$ and $\underset{\sim}{E}_s = -(1/c)\partial \underset{\sim}{A}_s/\partial t$. The amplitude $\hat{a}_s(z,t)$ in Eq.(2) is related to the magnetic field amplitude $\hat{B}_s(z,t)$ of the primary electromagnetic wave by $\hat{a}_s = e\hat{B}_s/mc^2k_s$. In the present analysis, it is assumed that the primary electromagnetic wave in Eq.(2) has evolved to finite amplitude following a phase of linear FEL instability. Moreover, although the (dimensionless) amplitude $\hat{a}_s$ is treated as finite, it should be noted that $\hat{a}_s << 1$ in the regimes of practical interest.

A detailed investigation of the sideband instability simplifies considerably if the analysis is carried out in the ponderomotive frame moving with velocity [19-21]

$$v_p = \frac{\omega_s}{k_s + k_0} . \tag{3}$$

Therefore, the subsequent analysis is carried out in ponderomotive-frame variables (z',t',γ') defined by the Lorentz transformation

$$\begin{aligned} z' &= \gamma_p(z - v_p t) , \\ t' &= \gamma_p(t - v_p z/c^2) , \\ \gamma' &= \gamma_p(\gamma - v_p p_z/mc^2), \end{aligned} \tag{4}$$

where $\gamma_p = (1 - v_p^2/c^2)^{-\frac{1}{2}}$, $\gamma' mc^2 = (m^2c^4 + c^2p_x'^2 + c^2p_y'^2 + c^2p_z'^2)^{\frac{1}{2}}$ is the mechanical energy, and the components of momentum (p_x',p_y',p_z') are related to the velocity $\underset{\sim}{v}' = d\underset{\sim}{x}'/dt'$ by $\underset{\sim}{p}' = \gamma' m\underset{\sim}{v}'$. We introduce the complex representation of the vector potentials defined by

$$\begin{aligned} \bar{a}_w(z) &= a_{xw}(z) - ia_{yw}(z) , \\ \bar{a}_s(z,t) &= a_{xs}(z,t) - ia_{ys}(z,t) , \end{aligned} \tag{5}$$

Making use of Eqs.(1) and (2) and the inverse transformation $z = \gamma_p(z' + v_p t')$ and $t = \gamma_p(t' + v_p z'/c^2)$, it is readily shown that

$$\begin{aligned} \bar{a}_w(z',t') &= -a_w \exp[-i\gamma_p k_0(z' + v_p t')] \ , \\ \bar{a}_s(z',t') &= \hat{a}_s(z',t')\exp[i(k_s' z' - \omega_s' t') + i\delta_s'(z',t')] \ , \end{aligned} \tag{6}$$

in ponderomotive-frame variables. Here, (ω_s', k_s') in the ponderomotive frame is related to (ω_s, k_s) in the laboratory frame by

$$\begin{aligned} \omega_s' &= \gamma_p(\omega_s - k_s v_p) \ , \\ k_s' &= \gamma_p(k_s - \omega_s v_p/c^2) \ . \end{aligned} \tag{7}$$

In general, we also allow for additional wave components with right-circular polarization. The corresponding complex vector potential $\bar{a}(z',t') = a_x(z',t') - ia_w(z',t')$ can then be expressed as

$$\bar{a}(z',t') = \sum_{k'} \hat{a}_{k'}(z',t')\exp[i(k'z' - \omega' t') + i\delta_{k'}'(z',t')] \ , \tag{8}$$

where (ω', k') in the ponderomotive frame is related to (ω, k) in the laboratory frame by

$$\begin{aligned} \omega' &= \gamma_p(\omega - k v_p) \ , \\ k' &= \gamma_p(k - \omega v_p/c^2) \ . \end{aligned} \tag{9}$$

Here, $k' = 2\pi n'/L'$, where L' is the fundamental periodicity length in the ponderomotive frame, and the summation $\sum_{k'}$ extends from $n' = -\infty$ to $n' = \infty$. Without loss of generality, we take $L' = 2\pi/k_p'$, where $k_p' = (k_s + k_0)/\gamma_p$. Comparing Eqs.(6) and (8), it is evident that the primary electromagnetic wave (ω_s', k_s') corresponds to one particular wave component in Eq.(8) with

$(\omega',k') = (\omega'_s,k'_s)$. For future reference, Eq.(8) can also be expressed as

$$a^-(z',t') = \sum_{k'} a_{k'}(z',t')\exp[i(k'z' - \omega't')] \ , \tag{10}$$

where the complex amplitude $a_{k'}(z',t')$ is defined by

$$a_{k'}(z',t') = \hat{a}_{k'}(z',t')\exp[i\delta'_{k'}(z',t')] \ . \tag{11}$$

We denote the axial position and energy of the j'th electron in the ponderomotive frame by $z'_j(t')$ and $\gamma'_j(t')$. In addition, it is assumed that all electrons move on surfaces with zero transverse canonical momentum, i.e., $P'_{xj} = 0 = P'_{yj}$. This gives for the transverse velocities $v'_{xj} = p'_{xj}/\gamma'_j m$ and $v'_{yj} = p'_{yj}/\gamma'_j m$,

$$\begin{aligned} v'_{xj} &= \frac{c}{\gamma'_j}\left[a_{xw}(z'_j,t') + a_x(z'_j,t')\right] \ , \\ v'_{yj} &= \frac{c}{\gamma'_j}\left[a_{yw}(z'_j,t') + a_y(z'_j,t')\right]. \end{aligned} \tag{12}$$

Making use of Eqs.(6), (10) and (12), it is straightforward to show that the microscopic current $J^-_M(z',t') = J_{xM}(z',t') - iJ_{yM}(z',t')$ can be expressed as

$$\begin{aligned} J^-_M(z',t') &= -e\sum_j (v'_{xj} - iv'_{yj})\delta[z' - z'_j(t')] \\ &= -ec\sum_j \frac{1}{\gamma'_j}\Big\{-a_w\exp[\gamma_p k_0(z' + v_p t')] \\ &\quad + \sum_{k'} a_{k'}(z',t')\exp[i(k'z' - \omega't')]\Big\}\delta[z' - z'_j(t')] \ , \end{aligned} \tag{13}$$

where $\sum_j$ denotes summation over electrons. For future reference, we also simplify the expression for $\gamma'_j = (1 + p'^2_{xj}/m^2c^2 + p'^2_{yj}/m^2c^2 + p'^2_{zj}/m^2c^2)^{\frac{1}{2}}$, where

$p'_{xj} = \gamma'_j m v'_{xj}$ and $p'_{yj} = \gamma'_j m v'_{yj}$ are defined in Eq.(12). Some straightforward algebra that makes use of Eqs.(6), (10) and (12) gives

$$\gamma'^2_j = 1 + \frac{p'^2_{zj}}{m^2c^2} + a_w^2 + \sum_{k'} |\hat{a}_{k'}|^2 - 2a_w \mathrm{Re}\left[\sum_{k'} a_{k'} \exp(i\theta'_j)\right] . \tag{14}$$

Here, the orbital phase factor $\theta'_j(t')$ is defined by

$$\theta'_j(t') = (k' + \gamma_p k_0) z'_j(t') - (\omega' - \gamma_p k_0 v_p) t' . \tag{15}$$

In the regimes of practical interest, a_w^2 is order unity, and $|\hat{a}_{k'}|^2 << 1$ for the electromagnetic wave components. Therefore, an excellent approximation to Eq.(14) is

$$\gamma'^2_j = 1 + \frac{p'^2_{zj}}{m^2c^2} + a_w^2 - 2a_w \mathrm{Re}\left[\sum_{k'} a_{k'} \exp(i\theta'_j)\right] , \tag{16}$$

where $a_{k'} = \hat{a}_{k'} \exp(i\delta'_{k'})$ is the complex wave amplitude. In Sec. III, we will make use of the form of γ'_j in Eq.(16) to investigate the equations of motion in the ponderomotive frame.

In the ponderomotive frame, Maxwell's equations for the complex vector potential $a^-(z',t') = a_x(z',t') - i a_y(z',t')$ associated with the average electromagnetic fields can be expressed as

$$\left(\frac{1}{c^2}\frac{\partial^2}{\partial t'^2} - \frac{\partial^2}{\partial z'^2}\right) a^-(z',t') = -\frac{4\pi e^2}{mc^3} \left\langle \sum_j (v'_{xj} - i v'_{yj}) \delta[z' - z'_j(t')] \right\rangle , \tag{17}$$

where $\langle \cdots \rangle$ denotes ensemble average. Making use of Eqs.(10) and (13), it follows that Eq.(17) can be expressed in the equivalent form

$$\sum_{k'}\left\{\left(-\frac{\omega'^2}{c^2}+k'^2\right)a_{k'}+\left(\frac{1}{c^2}\frac{\partial^2 a_{k'}}{\partial t'^2}-\frac{\partial^2 a_{k'}}{\partial z'^2}\right)\right.$$
$$\left.-\frac{2i\omega'}{c^2}\left(\frac{\partial a_{k'}}{\partial t'}+\frac{c^2k'}{\omega'}\frac{\partial a_{k'}}{\partial z'}\right)\right\}\exp[i(k'z'-\omega't')]$$
$$=-\frac{4\pi e^2}{mc^2}\sum_{k'}\left\langle\sum_j\frac{1}{\gamma'_j}a_{k'}\exp[i(k'z'-\omega't')]\delta[z'-z'_j(t')]\right\rangle \tag{18}$$
$$+\frac{4\pi e^2 a_w}{mc^2}\left\langle\sum_j\frac{1}{\gamma'_j}\exp[-ik_0\gamma_p(z'+v_pt')]\delta[z'-z'_j(t')]\right\rangle .$$

Consistent with the assumption that the amplitudes $a_{k'}$ are slowly varying with z' and t', we neglect the second-derivative contributions with respect to z' and t' in Eq.(18) but retain the terms proportional to $\partial a_{k'}/\partial t'$ and $\partial a_{k'}/\partial z'$ (Eikonal approximation).[32] Furthermore, we operate on Eq.(18) with $\int_0^{L'}\frac{dz'}{L'}\times \exp(-ik'z'+i\omega't')\cdots$, where L' is the fundamental periodicity length for the (fast) spatial oscillations in the ponderomotive frame. Treating the spatial variation of $a_{k'}$ and γ'_j as slow, the wave equation (18) then gives

$$\left\{\left(-\frac{\omega'^2}{c^2}+k'^2+\frac{4\pi e^2}{mc^2}\frac{1}{L'}\left\langle\sum_j\frac{1}{\gamma'_j}\right\rangle\right)a_{k'}\right.$$
$$\left.-\frac{2i\omega'}{c^2}\left(\frac{\partial a_{k'}}{\partial t'}+\frac{k'c^2}{\omega'}\frac{\partial a_{k'}}{\partial z'}\right)\right\} \tag{19}$$
$$=\frac{4\pi e^2 a_w}{mc^2}\frac{1}{L'}\left\langle\sum_j\frac{\exp(-i\theta'_j)}{\gamma'_j}\right\rangle$$

for the evolution of the k''th Fourier component. Here, $\theta'_j=(k'+\gamma_pk_0)z'_j(t')-(\omega'-\gamma_pk_0v_p)t'$ is the orbital phase defined in Eq.(15).

Separating Eq.(19) into fast and slow contributions gives

$$\omega'^2 = c^2 k'^2 + \frac{4\pi e^2}{m} \frac{1}{L'} \left\langle \sum_j \frac{1}{\gamma_j'} \right\rangle , \tag{20}$$

and

$$\frac{2i\omega'}{c^2} \left(\frac{\partial a_{k'}}{\partial t'} + \frac{k'c^2}{\omega'} \frac{\partial a_{k'}}{\partial z'} \right) = - \frac{4\pi e^2 a_w}{mc^2} \frac{1}{L'} \left\langle \sum_j \frac{\exp(-i\theta_j')}{\gamma_j'} \right\rangle . \tag{21}$$

Equation (20) determines the real oscillation frequency ω' in terms of k' and beam dielectric effects (proportional to $\langle \sum_j 1/\gamma_j' \rangle$). On the other hand, Eq.(21) describes the (slow) evolution of the complex amplitude $a_{k'}(z',t')$ induced by the wiggler field a_w. Expressing $a_{k'} = \hat{a}_{k'} \exp(i\delta_{k'}')$, the wave equation (21) can be separated into real and imaginary parts. This gives separate equations for the evolution of $\hat{a}_{k'}(z',t')$ and $\delta_{k'}'(z',t')$, i.e.,

$$2\omega' \left(\frac{\partial}{\partial t'} + \frac{k'c^2}{\omega'} \frac{\partial}{\partial z'} \right) \hat{a}_{k'} = \frac{4\pi e^2 a_w}{m} \frac{1}{L'} \left\langle \sum_j \frac{\sin(\theta_j' + \delta_{k'}')}{\gamma_j'} \right\rangle , \tag{22}$$

$$2\omega' \hat{a}_{k'} \left(\frac{\partial}{\partial t'} + \frac{k'c^2}{\omega'} \frac{\partial}{\partial z'} \right) \delta_{k'}' = \frac{4\pi e^2 a_w}{m} \frac{1}{L'} \left\langle \sum_j \frac{\cos(\theta_j' + \delta_{k'}')}{\gamma_j'} \right\rangle . \tag{23}$$

Equations (22) and (23) are fully equivalent to the (complex) wave equation (21).

We summarize here several noteworthy points regarding the wave equations (22) and (23) [or, equivalently, Eq.(21)].

(a) First, the orbits $z_j'(t')$ and $\gamma_j'(t')$ occurring in Eqs.(22) and (23) are determined self-consistently in terms of the wiggler and electromagnetic fields (Sec. III). Therefore, generally speaking, Eqs.(22) and (23) are

nonlinear equations for the evolution of $\hat{a}_{k'}$ and $\delta'_{k'}$. Indeed, Eqs.(22) and (23), together with the dynamical equations for $z'_j(t')$ and $\gamma'_j(t')$, can form the basis for numerical simulations of the nonlinear evolution of the wave spectrum and the sideband instability.

(b) Second, for $(\omega',k') = (\omega'_s,k'_s)$, Eqs.(22) and (23) describe the evolution of the primary electromagnetic wave $(\hat{a}_s,\delta'_s)$. In particular, $\hat{a}_s(z',t')$ and $\delta'_s(z',t')$ evolve according to

$$2\omega'_s\left(\frac{\partial}{\partial t'} + \frac{k'_s c^2}{\omega'_s}\frac{\partial}{\partial z'}\right)\hat{a}_s = \frac{4\pi e^2 a_w}{m}\frac{1}{L'}\left\langle \sum_j \frac{\sin(\theta'_{js} + \delta'_s)}{\gamma'_j} \right\rangle , \tag{24}$$

$$2\omega'_s\hat{a}_s\left(\frac{\partial}{\partial t'} + \frac{k'_s c^2}{\omega'_s}\frac{\partial}{\partial z'}\right)\delta'_s = \frac{4\pi e^2 a_w}{m}\frac{1}{L'}\left\langle \sum_j \frac{\cos(\theta'_{js} + \delta'_s)}{\gamma'_j} \right\rangle , \tag{25}$$

where (ω'_s,k'_s) solves Eq.(20), and θ'_{js} is defined by

$$\theta'_{js} = k'_p z'_j(t') . \tag{26}$$

Here, use has been made of $\omega'_s - \gamma_p k_0 v_p = \gamma_p[\omega_s - (k_s + k_0)v_p] = 0$, and k'_p is defined by $k'_p = (k'_s + \gamma_p k_0) = \gamma_p\,(k_s + k_0 - \omega_s v_p/c^2) \equiv (k_s + k_0)/\gamma_p$.

(c) If, in addition, there are secondary electromagnetic wave components $(\hat{a}_{k'},\delta'_{k'})$ with frequency and wavenumber (ω',k') different from (ω'_s,k'_s), then $\hat{a}_{k'}(z',t')$ and $\delta'_{k'}(z',t')$ evolve according to Eqs.(22) and (23), where (ω',k') solves Eq.(20), and $\theta'_j = (k' + \gamma_p k_0)z'_j(t') - (\omega' - \gamma_p k_0 v_p)t'$ is defined in Eq.(15).

(d) Finally, there is some latitude in specifying the precise operational meaning of the statistical averages $\left\langle \sum_j \cdots \right\rangle$ occurring in the wave equations (22) and (23). For present purposes, let us assume that the orbits

$z_j'(t')$ and $\gamma_j'(t')$ have been calculated in terms of the initial values $z_j'(0)$ and $\gamma_j'(0)$. Then the simplest definition of the statistical average $\left\langle \sum_j \cdots \right\rangle$ over some phase function $\psi\left(\theta_j'(0),\gamma_j'(0)\right)$ is given by

$$\frac{1}{L'}\left\langle \sum_j \psi\left(\theta_j'(0),\gamma_j'(0)\right)\right\rangle \tag{27}$$

$$= \hat{n}_b' \int_0^{2\pi} \frac{d\theta_0'}{2\pi} \int_1^{\infty} d\gamma_0' G(\theta_0',\gamma_0')\psi(\theta_0',\gamma_0') \ .$$

Here, $\hat{n}_b'$ is the average density of the beam electrons in the ponderomotive frame, and $G(\theta_0',\gamma_0')$ is the (probability) distribution of electrons in initial phase θ_0' and energy γ_0'.

III. PARTICLE ORBIT EQUATIONS

We now obtain the orbit equations for $z'_j(t')$ and $\gamma'_j(t')$. In the ponderomotive frame, the equation of motion for $p'_{zj}(t') = \gamma'_j(t')mdz'_j/dt'$ is

$$\frac{d}{dt'} p'_{zj} = -mc^2 \frac{\partial}{\partial z'_j} \gamma'_j \ . \tag{28}$$

Here, to the level of accuracy required in the present analysis, γ'_j is defined in terms of p'_{zj} and field quantities by Eq.(16). Neglecting the variation of $a_{k'}(z'_j,t')$ with respect to z'_j in comparison with $\partial\theta'_j/\partial z'_j = (k' + \gamma_p k_0)$, it readily follows from Eqs.(16) and (28) that $z'_j(t')$ evolves according to

$$\frac{d^2}{dt'^2} z'_j + \frac{1}{\gamma'_j} \frac{d\gamma'_j}{dt'} \frac{dz'_j}{dt'} = - \frac{c^2 a_w}{\gamma'^2_j} \mathrm{Im}\left(\sum_{k'} (k' + \gamma_p k_0) a_{k'} \exp(i\theta'_j) \right) \ , \tag{29}$$

where $a_{k'} = \hat{a}_{k'} \exp(i\delta'_{k'})$, and $\theta'_j = (k' + \gamma_p k_0)z'_j - (\omega' - \gamma_p k_0 v_p)t'$. In Eq.(29), the summation $\sum_{k'}$ includes the primary electromagnetic wave (ω'_s, k'_s) as well as other electromagnetic wave components.

With regard to the evolution of $\gamma'_j(t')$, we make use of

$$\begin{aligned} \frac{d}{dt'} \gamma'_j &= - \frac{e}{mc^2} \underset{\sim}{v}'_j \cdot \underset{\sim}{E} \\ &= \frac{(\underset{\sim}{a}_w + \underset{\sim}{a})}{\gamma'_j} \cdot \frac{\partial}{\partial t'} (\underset{\sim}{a}_w + \underset{\sim}{a}) \\ &= \frac{1}{2\gamma'_j} \frac{\partial}{\partial t'} \left\{ \left[a_{xw}(z'_j,t') + a_x(z'_j,t') \right]^2 + \left[a_{yw}(z'_j,t') + a_y(z'_j,t') \right]^2 \right\} , \end{aligned} \tag{30}$$

where (a_{xw}, a_{yw}) denotes the vector potential for the wiggler field [Eq.(6)], and (a_x, a_y) denotes the vector potential for the electromagnetic wave contributions [Eq.(8)]. In obtaining Eq.(30), use has been made of Eq.(12) to

express the perpendicular velocity (v'_{xj},v'_{yj}) in terms of field quantities. Substituting Eqs.(6) and (8) into Eq.(33) and making use of $a_w^2 = \text{const.}$ gives

$$\frac{d}{dt'}\gamma'_j = \frac{1}{2\gamma'_j}\frac{\partial}{\partial t'}\left[\sum_{k'}\left(|\hat{a}_{k'}|^2 - 2a_w \text{Re}\left[a_{k'}\exp(i\theta'_j)\right]\right)\right] , \tag{31}$$

where $a_{k'} = \hat{a}_{k'}\exp(i\delta'_{k'})$. Neglecting $|\hat{a}_{k'}|^2$ in comparison with $2a_w a_{k'}$ in Eq.(31), and treating $a_{k'}(z',t')$ as slowly varying with respect to t' in comparison with $\partial\theta'_j/\partial t' = -(\omega' - \gamma_p k_0 v_p)$, it is straightforward to show that Eq.(31) can be approximated by

$$\frac{d}{dt'}\gamma'_j = -\frac{a_w}{\gamma'_j}\,\text{Im}\left(\sum_{k'}(\omega' - \gamma_p k_0 v_p)a_{k'}\exp(i\theta'_j)\right) , \tag{32}$$

where $\theta'_j = (k' + \gamma_p k_0)z'_j - (\omega' - \gamma_p k_0 v_p)t'$. Equation (32) can be used to eliminate $d\gamma'_j/dt'$ in the equation of motion for $z'_j(t')$ in Eq.(29). This readily gives

$$\frac{d^2}{dt'^2}z'_j = -\frac{c^2 a_w}{\gamma_j'^2}\,\text{Im}\left[\sum_{k'}\left((k' + \gamma_p k_0) - \frac{(\omega' - \gamma_p k_0 v_p)}{c^2}\frac{dz'_j}{dt'}\right) \times a_{k'}\exp(i\theta'_j)\right] . \tag{33}$$

Equations (32) and (33) are the final equations of motion used in the present analysis. Note that Eqs.(32) and (33) generally allow for several wave components. Moreover, it should be kept in mind that the slow variation of $a_{k'}(z',t')$ with respect to z' and t' have been neglected in deriving Eqs.(32) and (33). For future reference, we now specialize to the case where there is a single wave component $(\omega',k') = (\omega'_s,k'_s)$ corresponding to the primary electromagnetic wave $(\hat{a}_s,\delta'_s)$. Making use of $\omega'_s = \gamma_p(\omega_s - k_s v_p) \equiv \gamma_p k_0 v_p$ and $k'_s + \gamma_p k_0 = \gamma_p(k_s + k_0 - \omega_s v_p/c^2) = (k_s + k_0)/\gamma_p \equiv k'_p$, it is readily shown that Eqs.(32) and (33) reduce to

$$\frac{d}{dt'}\gamma_j' = 0 \tag{34}$$

$$\frac{d^2}{dt'^2}\theta_{js}' + \frac{c^2 a_w k_p'^2}{\gamma_j'^2}\,\mathrm{Im}\left[a_s \exp(i\theta_{js}')\right] = 0\ , \tag{35}$$

for the case of a single wave component (ω_s', k_s'). Here, $\theta_{js}' = k_p' z_j'(t')$ and $a_s = \hat{a}_s \exp(i\delta_s')$. To the level of accuracy which neglects $\partial a_s/\partial t'$ in Eq.(31), we note from Eq.(34) that energy is conserved in the ponderomotive frame (γ_j' = const.). The concomitant simplification in the particle orbits and related analysis is the primary motivation for carrying out the present investigations in the ponderomotive frame.[19-21]

IV. SIDEBAND INSTABILITY - MODEL AND DEFINITIONS

Assuming a single electromagnetic wave component (ω_s', k_s'), in Secs. V and VI, we make use of the coupled equations for $\hat{a}_s(z',t')$ [Eq.(24)], $\delta_s(z',t')$ [Eq.(25)], and $\theta_{js}'(t')$ [Eq.(35)] to investigate detailed properties of the sideband instability in circumstances where the electrons are deeply trapped in the ponderomotive potential. In particular, we examine linear stability properties for small-amplitude perturbations $(\delta\hat{a}_s, \tilde{\delta}_s')$ about a finite-amplitude state $(\hat{a}_s^0, \delta_s^0)$. In this regard, two cases are distinguished.

A. Perturbations about a primary electromagnetic wave equilibrium with constant phase δ_s^0 and constant amplitude $\hat{a}_s^0 (\partial/\partial t' = 0 = \partial/\partial z')$. Previous kinetic studies[19-21] of the sideband instability based on the Vlasov-Maxwell equations have shown that both trapped and untrapped electrons are required for such an equilibrium state to exist.

B. Perturbations about a quasi-steady primary electromagnetic wave with phase δ_s^0 which is slowly varying with z'. Previous single-particle analyses[32-42] of the sideband instability have emphasized this case, assuming that <u>all</u> of the electrons are trapped, or that the untrapped electrons play no role in sustaining the primary electromagnetic wave.

The sideband instability is investigated for Cases A and B in Secs. V and VI, respectively. The analysis shows that detailed stability properties differ substantially in the two case (e.g., the scaling of the growth rate with beam current, primary wave amplitude, etc.). This difference is clearly associated with the assumptions regarding the equilibrium state and the role of the untrapped electrons.

Although the dispersion relation (20) incorporates beam dielectric effects through the term $(4\pi e^2/mL')\left\langle \sum_j \gamma_j'^{-1} \right\rangle$, for present purposes we

assume a very tenuous electron beam and approximate Eq.(20) by $\omega_s^2 = c^2k_s^2$ for the primary electromagnetic wave. Assuming a forward-moving electromagnetic wave, we solve the simultaneous resonance conditions

$$\omega_s = +ck_s \ , \qquad \omega_s = (k_s + k_0)v_p \ , \tag{36}$$

for ω_s and k_s. This readily gives the familiar results

$$\omega_s = \gamma_p^2(1 + v_p/c)k_0v_p \ , \qquad k_s = \gamma_p^2(1 + v_p/c)(v_p/c)k_0 \ , \tag{37}$$

where $\gamma_p^2 = (1 - v_p^2/c^2)^{-\frac{1}{2}}$, and $v_p = \omega_s/(k_s + k_0)$ is (nearly) synchronous with the average axial velocity V_b of the beam electrons. Moreover, from Eq.(37), the ponderomotive wavenumber $k_p' = (k_s + k_0)/\gamma_p$ can be expressed as

$$k_p' = \gamma_p(1 + v_p/c)k_0 \ . \tag{38}$$

For future reference, we introduce the small dimensionless parameter Γ_0^3 and the bounce frequency $\hat{\omega}_B(\gamma_j')$ of the trapped electrons defined by

$$\Gamma_0^3 = \frac{1}{4}\frac{a_w^2}{\hat{\gamma}'^3}\frac{\hat{\omega}_{pT}^2}{\gamma_p^2c^2k_0^2}\frac{(1 + v_p/c)}{v_p/c} \ll 1 \ , \tag{39}$$

and

$$\hat{\omega}_B(\gamma_j') = (c^2k_p'^2a_w\hat{a}_s^0/\gamma_j'^2)^{\frac{1}{2}} \ . \tag{40}$$

In Eq.(39), the characteristic energy $\hat{\gamma}'$ of an electron trapped in the ponderomotive potential is given approximately by

$$\hat{\gamma}' = (1 + a_w^2)^{\frac{1}{2}} \ . \tag{41}$$

[See Eq.(14) with $p_{zj}' = 0$ and $|a_s| \ll a_w$.] Moreover, $\hat{\omega}_{pT}^2 = 4\pi\hat{n}_T'e^2/m = 4\pi\hat{n}_Te^2/\gamma_pm$

is the plasma frequency-squared of the trapped electrons, and $\hat{n}_T' = \hat{n}_T/\gamma_p$ is the average density in the ponderomotive frame. In Eq.(40), $\hat{\omega}_B(\gamma_j')$ is the bounce frequency (in the ponderomotive frame) of an electron with energy γ_j' trapped near the bottom of the ponderomotive potential. For $\gamma_j' = \hat{\gamma}'$, the bounce frequency Ω_B in the laboratory frame is defined by

$$\begin{aligned} \Omega_B &= \hat{\omega}_B(\hat{\gamma}')/\gamma_p \\ &= (c^2 k_p'^2 a_w \hat{a}_s^0/\hat{\gamma}'^2\gamma_p^2)^{\frac{1}{2}} \end{aligned} \tag{42}$$

for deeply trapped electrons. In Eq.(42), k_p' and $\hat{\gamma}'$ are defined for a tenuous electron beam by $k_p' = (k_s + k_0)/\gamma_p = \gamma_p(1 + v_p/c)k_0$ and $\hat{\gamma}' = (1 + a_w^2)^{\frac{1}{2}}$. Therefore, Eq.(42) can be expressed in the equivalent (and more familiar) form

$$\Omega_B = \left(1 + \frac{v_p}{c}\right)\left(\frac{a_w \hat{a}_s^0}{1 + a_w^2}\right)^{\frac{1}{2}} ck_0 \, .$$

V. SIDEBAND INSTABILITY FOR PRIMARY ELECTROMAGNETIC WAVE WITH CONSTANT PHASE AND AMPLITUDE

We now make use of Eqs.(24), (25) and (35) to investigate detailed properties of the sideband instability for small-amplitude perturbations about a primary electromagnetic wave with constant amplitude $\hat{a}_s^0$ and phase δ_s^0. Each quantity is expressed as its equilibrium value plus a perturbation, i.e.,

$$\hat{a}_s = \hat{a}_s^0 + \delta\hat{a}_s \ ,$$

$$\delta_s' = \delta_s^0 + \tilde{\delta}_s' \ , \tag{43}$$

$$\theta_{js}' = \theta_{js}^0 + \delta\theta_{js}' \ ,$$

where $\theta_{js}^0(t') = k_p' z_{j0}'(t')$ and $\delta\theta_{js}'(t') = k_p'\delta z_j'(t')$. In the ponderomotive frame, γ_j' = const. follows from Eq.(34) to the level of accuracy in the present analysis.

A. Equilibrium Model

Making use of Eqs.(24) and (25), it follows that $\hat{a}_s^0$ and δ_s^0 generally evolve according to

$$2\omega_s'\left(\frac{\partial}{\partial t'} + \frac{k_s'c^2}{\omega_s'}\frac{\partial}{\partial z'}\right)\hat{a}_s^0 = \frac{4\pi e^2 a_w}{m}\frac{1}{L'}\left\langle \sum_j \frac{\sin(\theta_{js}^0 + \delta_s^0)}{\gamma_j'} \right\rangle \ , \tag{44}$$

$$2\omega_s'\hat{a}_s^0\left(\frac{\partial}{\partial t'} + \frac{k_s'c^2}{\omega_s'}\frac{\partial}{\partial z'}\right)\delta_s^0 = \frac{4\pi e^2 a_w}{m}\frac{1}{L'}\left\langle \sum_j \frac{\cos(\theta_{js}^0 + \delta_s^0)}{\gamma_j'} \right\rangle \ . \tag{45}$$

Moreover, $\theta_{js}^0(t') = k_p' z_{j0}'(t')$ solves Eq.(35) with all perturbations set equal to zero, i.e., $\delta\hat{a}_s = 0$, $\tilde{\delta}_s' = 0$ and $\delta z_j' = 0$. That is, $\theta_{js}^0(t')$ solves the pendulum equation

$$\frac{d^2}{dt'^2}\,\theta_{js}^0 + \hat{\omega}_B^2(\gamma_j')\sin(\theta_{js}^0 + \delta_s^0) = 0 \quad , \tag{46}$$

where $\hat{\omega}_B(\gamma_j') = (c^2 k_p'^2 a_w \hat{a}_s^0/\gamma_j'^2)^{\frac{1}{2}}$ is the bounce frequency of electrons trapped near the bottom of the ponderomotive potential.

If δ_s^0 and $\hat{a}_s^0$ are initially constant (independent of z' and t' at t' = 0), then it follows from Eqs.(44) and (45) that

$$\begin{aligned} \hat{a}_s^0 &= \text{const.}, \\ \delta_s^0 &= \text{const.}, \end{aligned} \tag{47}$$

for all z' and t' provided

$$\left\langle \sum_j \frac{\sin(\theta_{js}^0 + \delta_s^0)}{\gamma_j'} \right\rangle = 0 = \left\langle \sum_j \frac{\cos(\theta_{js}^0 + \delta_s^0)}{\gamma_j'} \right\rangle . \tag{48}$$

To satisfy Eq.(48) necessarily requires that the distribution of beam electrons have both untrapped- and trapped-electron components. For example, the condition $\left\langle \sum_j \gamma_j'^{-1}\cos(\theta_{js}^0 + \delta_s^0) \right\rangle = 0$ cannot be satisfied if <u>all</u> of the electrons are deeply trapped with $\theta_{js}^0 + \delta_s^0 \simeq 0$. We also note that Eqs.(47) and (48) are analogous to the equilibrium constraints assumed by Davidson et. al.[19-21] in recent kinetic studies of the sideband instability.

Without loss of generality, in the remainder of Sec. V we take $\delta_s^0 = 0$ and rewrite Eq.(48) in the equivalent form

$$\left\langle \sum_j \frac{\exp(-i\theta_{js}^0)}{\gamma_j'} \right\rangle = 0 . \tag{49}$$

For $\delta_s^0 = 0$ and $\hat{a}_s^0 = \text{const.}$, the equilibrium orbit equation (46) can be expressed as

$$\frac{d^2}{dt'^2}\theta_{js}^0 + \hat{\omega}_B^2(\gamma_j')\sin(\theta_{js}^0) = 0 \tag{50}$$

where $\hat{\omega}_B(\gamma_j') = (c^2 k_p'^2 a_w \hat{a}_s^0/\gamma_j'^2)^{\frac{1}{2}} = \text{const.}$ A detailed analysis of Eq.(50) shows that the electron motion is untrapped for energies γ_j' satisfying (Fig. 1)

$$\gamma_j' > \hat{\gamma}_+' \equiv \left[1 + (a_w + \hat{a}_s^0)^2\right]^{\frac{1}{2}} . \tag{51}$$

[Here, $a_w > 0$ and $\hat{a}_s^0 > 0$ have been assumed without loss of generality.] That is, when Eq.(51) is satisfied, the particle motion is modulated by the ponderomotive potential, but the normalized velocity $d\theta_{js}^0/dt'$ does not change polarity (Fig. 1). On the other hand, for $\gamma_j' < \hat{\gamma}_+'$, the electrons are trapped, and the motion described by Eq.(50) is cyclic, corresponding to periodic motion in the ponderomotive potential. From Eq.(50), it is readily shown that the minimum allowable energy of a trapped electron is

$$\hat{\gamma}_-' \equiv \left[1 + (a_w - \hat{a}_s^0)^2\right]^{\frac{1}{2}} . \tag{52}$$

Because $\hat{a}_s^0 << a_w$ in the regimes of practical interest, we note from Eqs.(51) and (52) that the characteristic energy of a trapped electron is approximately $\hat{\gamma}' \equiv (1 + a_w^2)^{\frac{1}{2}}$ [Eq.(41)].

B. Linearized Equations

We now investigate stability properties for small-amplitude perturbations about the equilibrium state described by Eqs.(47), (49) and (50). In this regard, it is convenient to work directly with Eq.(21) for the evolution of the complex amplitude $a_s = \hat{a}_s \exp(i\delta_s')$. Expressing $a_s = a_s^0 + \delta a_s$ and $\theta_{js}' = \theta_{js}^0 + \delta\theta_{js}'$, Eq.(21) gives

$$2i\omega_s'\left(\frac{\partial}{\partial t'} + \frac{c^2 k_s'}{\omega_s'}\frac{\partial}{\partial z'}\right)(a_s^0 + \delta a_s)$$
$$= -\frac{4\pi e^2 a_w}{m}\frac{1}{L'}\left\langle \sum_j \frac{\exp(-i\theta_{js}^0 - i\delta\theta_{js}')}{\gamma_j'} \right\rangle . \tag{53}$$

Making use of $a_s^0 = \text{const.}$ [Eq.(47)] and $\left\langle \sum_j \exp(-i\theta_{js}^0)/\gamma_j' \right\rangle = 0$ [Eq.(49)], and Taylor expanding $\exp(-i\delta\theta_{js}') = (1 - i\delta\theta_{js}')$ on the right-hand side of Eq.(53), we obtain

$$2\omega_s'\left(\frac{\partial}{\partial t'} + \frac{c^2 k_s'}{\omega_s'}\frac{\partial}{\partial z'}\right)\delta a_s = \frac{4\pi e^2 a_w}{m}\frac{1}{L'}\left\langle \sum_j \frac{\exp(-i\theta_{js}^0)}{\gamma_j'}\,\delta\theta_{js}' \right\rangle \tag{54}$$

for the evolution of the complex amplitude δa_s. Here, $\delta a_s = \delta\hat{a}_s + i\tilde{\delta}_s'\hat{a}_s^0$ for small-amplitude perturbations, where $\delta_s^0 = 0$ is assumed. In Eq.(54), the perturbed orbit $\delta\theta_{js}'(t') = k_p'\delta z_j'(t')$ is calculated from Eq.(35). Linearizing Eq.(35) about the equilibrium orbit equation (50) readily gives

$$\frac{d^2}{dt'^2}\,\delta\theta_{js}' + \hat{\omega}_B^2(\gamma_j')\cos\left(\theta_{js}^0\right)\delta\theta_{js}' = -\frac{c^2 k_p'^2 a_w}{\gamma_j'^2}\,\mathrm{Im}\left[\delta a_s \exp(i\theta_{js}^0)\right] \quad . \tag{55}$$

Here, $\theta_{js}^0(t')$ solves Eq.(50), and Eq.(55) is generally valid for both untrapped and trapped electrons.

Equations (54) and (55) constitute coupled linearized equations for the complex amplitude δa_s and perturbed orbit $\delta\theta_{js}'$. For present purposes, it is useful to express

$$\delta\theta_{js}' = \delta\psi_{js}'\exp(i\theta_{js}^0) + \delta\psi_{js}'^*\exp(-i\theta_{js}^0) \ , \tag{56}$$

where $\delta\psi_{js}'^*$ denotes the complex conjugate of $\delta\psi_{js}'$. Making use of Eqs.(50), (55) and (56), it is readily shown that $\delta\psi_{js}'(t')$ evolves according to

$$\frac{d^2}{dt'^2}\,\delta\psi'_{js} + 2i\left(\frac{d\theta^0_{js}}{dt'}\right)\frac{d}{dt'}\,\delta\psi'_{js}$$

$$+\left[\hat{\omega}_B^2(\gamma'_j)\cos\left(\theta^0_{js}\right) - i\hat{\omega}_B^2(\gamma'_j)\sin\left(\theta^0_{js}\right) - \left(\frac{d\theta^0_{js}}{dt'}\right)^2\right]\delta\psi'_{js} \tag{57}$$

$$= -\frac{c^2k'^2_p a_w}{\gamma'^2_j}\,\frac{\delta a_s}{2i}\ .$$

Note in Eq.(56) that we have factored out the (fast) orbital variations in $\delta\theta'_{js}$ proportional to $\exp(\pm i\theta^0_{js})$. On the other hand, the amplitudes $\delta\psi'_{js}$ and $\delta\psi'^{*}_{js}$ in Eq.(56) describe the systematic variation of $\delta\theta'_{js}$ induced by the slowly changing wave perturbation δa_s [see Eq.(57)].

Substituting Eq.(56) into the right-hand side of Eq.(54) gives

$$\left\langle \sum_j \frac{\exp(-i\theta^0_{js})}{\gamma'_j}\,\delta\theta'_{js} \right\rangle$$

$$= \left\langle \sum_j \left[\frac{\delta\psi'_{js}}{\gamma'_j} + \frac{\delta\psi'^{*}_{js}}{\gamma'_j}\exp(-2i\theta^0_{js})\right] \right\rangle . \tag{58}$$

The term proportional to $\exp(-2i\theta^0_{js})$ in Eq.(58) generally has fast oscillatory contributions from the trapped and untrapped electrons. As in single-particle analyses with $\hat{a}^0_s = 0$, we assume that this term averages to zero in the statistical average $\left\langle \sum_j \cdots \right\rangle$. Equation (54) then becomes

$$2\omega'_s\left(\frac{\partial}{\partial t'} + \frac{c^2k'_s}{\omega'_s}\,\frac{\partial}{\partial z'}\right)\delta a_s = \frac{4\pi e^2 a_w}{m}\,\frac{1}{L'}\left\langle \sum_j \frac{\delta\psi'_{js}}{\gamma'_j} \right\rangle , \tag{59}$$

where the slow evolution of $\delta\psi'_{js}$ is determined in terms of δa_s from Eq.(57).

C. Sideband Instability

The coupled linearized equations (57) and (59) can be used to investigate detailed stability properties for a wide variety of untrapped- and trapped-electron populations. For present purposes, however, we focus on the sideband instability, assuming that the trapped electrons are deeply trapped near the bottom of the ponderomotive potential with energy $\gamma_j' \simeq \hat{\gamma}_-'$ [Eq.(52)] and average density $\hat{n}_T = \text{const}$. The t'- and z'-dependence of the wave perturbation δa_s is assumed to be of the form

$$\exp[-i(\Delta\omega')t' + i(\Delta k')z'] \quad , \tag{60}$$

where $\text{Im}(\Delta\omega') > 0$ corresponds to temporal growth. Approximating $\hat{\gamma}_-' \simeq (1 + a_w^2)^{\frac{1}{2}} \equiv \hat{\gamma}'$, the wave equation (59) becomes

$$-2i\omega_s'\left(\Delta\omega' - \frac{c^2k_s'}{\omega_s'}\Delta k'\right)\delta a_s = \frac{a_w\hat{\omega}_{pT}^2}{\hat{\gamma}'}\delta\psi_s' \tag{61}$$

for perturbation frequency $\Delta\omega'$ and wavenumber $\Delta k'$ characteristic of the trapped-electron motion. In Eq.(61), $\hat{\omega}_{pT}^2 = 4\pi\hat{n}_T'e^2/m = 4\pi\hat{n}_Te^2/\gamma_p m$, and the subscript j has been dropped from $\delta\psi_{js}'$. For deeply trapped electrons, it also follows that $\theta_{js}^0 \simeq 2n\pi$ $(n = 0, \pm1, \pm2, \cdots)$ and $d\theta_{js}^0/dt' \simeq 0$ in the linearized orbit equation (57). Therefore, Eq.(57) can be approximated by

$$\left[-(\Delta\omega')^2 + \hat{\omega}_B^2(\hat{\gamma}')\right]\delta\psi_s' = -\frac{c^2k_p'^2a_w}{\hat{\gamma}'^2}\frac{\delta a_s}{2i} \quad . \tag{62}$$

Combining Eqs.(61) and (62) readily gives the desired dispersion relation

$$\left(\Delta\omega' - \frac{c^2k_s'}{\omega_s'}\Delta k'\right)\left[(\Delta\omega')^2 - \hat{\omega}_B^2(\hat{\gamma}')\right] = \frac{a_w^2\hat{\omega}_{pT}^2c^2k_p'^2}{4\omega_s'\hat{\gamma}'^3} \quad , \tag{63}$$

which determines $\Delta\omega'$ in terms of $\Delta k'$ and other system parameters.

It is useful to transform $\Delta\omega'$ and $\Delta k'$ in Eq.(63) back to the laboratory frame, and introduce the small dimensionless parameter Γ_0^3 defined in Eq.(39). In this regard, making use of $\omega_s' = \gamma_p k_0 v_p$ and $k_p' = (k_s + k_0)/\gamma_p = \gamma_p(1 + v_p/c)k_0$ [Eq.(38)], the right-hand side of Eq.(63) is readily expressed as

$$\frac{a_w^2 \hat{\omega}_{pT}^2 c^2 k_p'^2}{4\omega_s' \hat{\gamma}'^3} = \gamma_p^3(1 + v_p/c)\Gamma_0^3 c^3 k_0^3 \ . \tag{64}$$

Moreover, it follows from Eq.(9) that

$$\begin{aligned} \Delta\omega' &= \gamma_p(\Delta\omega - v_p\Delta k) \ , \\ \Delta k' &= \gamma_p[\Delta k - (v_p/c^2)\Delta\omega] \ , \end{aligned} \tag{65}$$

where $\Delta\omega$ and Δk are the frequency and wavenumber of the perturbation in the laboratory frame. Consistent with neglecting beam dielectric effects (see Sec. IV), we approximate $\omega_s' = ck_s'$ and $\Delta\omega' - (c^2 k_s'/\omega_s')\Delta k' = \Delta\omega' - c\Delta k'$ on the left-hand side of Eq.(63). Making use of Eq.(65), it follows that

$$\Delta\omega' - c\Delta k' = \gamma_p(1 + v_p/c)\left[(\Delta\omega - v_p\Delta k) - ck_0 \frac{v_p}{c}\frac{\Delta k}{k_s}\right] \ , \tag{66}$$

where $k_s = \gamma_p^2(1 + v_p/c)(v_p/c)k_0$ is defined in Eq.(37). We further introduce the shorthand notation

$$\begin{aligned} \Delta\Omega &= \Delta\omega - v_p\Delta k \ , \\ \Delta K &= k_0 \frac{v_p}{c}\frac{\Delta k}{k_s} \ . \end{aligned} \tag{67}$$

Substituting Eqs.(64)-(67) into Eq.(63) then gives the dispersion relation

$$(\Delta\Omega - c\Delta K)\left[(\Delta\Omega)^2 - \Omega_B^2\right] = \Gamma_0^3 c^3 k_0^3 \ , \tag{68}$$

where $\Omega_B = (c^2 k_p'^2 a_w \hat{a}_s^0/\hat{\gamma}'^2\gamma_p^2)^{\frac{1}{2}}$ is the bounce frequency in the laboratory frame, and Γ_0^3 is defined in Eq.(39).

The dispersion relation (68) is equivalent to Eq.(63). Most striking is the fact that Eq.(68) is identical (neglecting beam dielectric effects) to the cubic limit of the kinetic dispersion relation[19,20] derived for deeply trapped electrons assuming constant equilibrium amplitude $\hat{a}_s^0$ and phase δ_s^0 of the primary electromagnetic wave (ω_s, k_s). Equation (68) is analyzed extensively in Ref. 20, where the growth rate $\mathrm{Im}(\Delta\Omega)$ and real oscillation frequency $\mathrm{Re}(\Delta\Omega)$ are calculated in terms of $c\Delta K$, Ω_B and $\Gamma_0 k_0 c$ over a wide range of system parameters. For present purposes, we summarize selected key results.

(a) A detailed investigation[20] of Eq. (68) over a wide range of system parameters shows that the maximum growth rate occurs for frequency and wavenumber in the vicinity of

$$\begin{aligned} \Delta\Omega &\approx -\Omega_B \ , \\ \Delta K &\approx -\Omega_B/c \ , \end{aligned} \tag{69}$$

Note that Eq.(69) corresponds to the lower sideband, which exhibits strong instability. [As discussed in Ref. 19, excitation of the lower sideband is associated with the assumption that the wave perturbation has (nearly) right-circular polarization. For wave perturbations with left-circular polarization, it is found[19] that the upper sideband exhibits instability.]

(b) We introduce the shifted frequency $\Delta\tilde{\Omega}$ and wavenumber $\Delta\tilde{K}$ defined by

$$\begin{aligned} \Delta\Omega &= -\Omega_B + \Delta\tilde{\Omega} \ , \\ \Delta K &= -\Omega_B/c + \Delta\tilde{K} \ . \end{aligned} \tag{70}$$

Making use of Eq.(70), the dispersion relation (68) can be expressed in the equivalent form

$$(\Delta\tilde{\Omega})(\Delta\tilde{\Omega} - 2\Omega_B)(\Delta\tilde{\Omega} - c\Delta\tilde{K}) = \Gamma_0^3 c^3 k_0^3 \ . \tag{71}$$

Because maximum growth is found[20] to occur for $\widetilde{\Delta K} \approx 0$, we solve Eq.(71) for the case $\widetilde{\Delta K} = 0$ exactly. The solution to $(\Delta\widetilde{\Omega})^3 - 2\Omega_B(\Delta\widetilde{\Omega})^2 - \Gamma_0^3 c^3 k_0^3 = 0$ then determines the characteristic maximum growth rate $\mathrm{Im}(\Delta\widetilde{\Omega}) = \mathrm{Im}(\Delta\omega)$. Some straightforward algebra gives[20]

$$\mathrm{Im}(\Delta\omega) = \Gamma_0 k_0 c \frac{(3)^{1/2}}{(2)^{5/3}} \left(1 + \frac{32}{27} \frac{\Omega_B^3}{\Gamma_0^3 k_0^3 c^3}\right)^{1/3} \tag{72}$$

$$\times \left\{\left[1 + \left(1 + \frac{32}{27} \frac{\Omega_B^3}{\Gamma_0^3 k_0^3 c^3}\right)^{-1/2}\right]^{2/3} - \left[1 - \left(1 + \frac{32}{27} \frac{\Omega_B^3}{\Gamma_0^3 k_0^3 c^3}\right)^{-1/2}\right]^{2/3}\right\}$$

for $\widetilde{\Delta K} = 0$.

(c) In the weak-pump regime ($\Omega_B << \Gamma_0 k_0 c$), Eq.(72) reduces to

$$\mathrm{Im}(\Delta\omega) = \frac{(3)^{1/2}}{2} \Gamma_0 k_0 c, \text{ for } \Omega_B << \Gamma_0 k_0 c \,. \tag{73}$$

On the other hand, in the strong-pump regime ($\Omega_B >> \Gamma_0 k_0 c$), Eq.(72) gives

$$\mathrm{Im}(\Delta\omega) = \frac{\Gamma_0 k_0 c}{(2)^{1/2}} \left(\frac{\Gamma_0 k_0 c}{\Omega_B}\right)^{1/2}, \text{ for } \Omega_B >> \Gamma_0 k_0 c \,. \tag{74}$$

Figure 2 shows a plot of $\mathrm{Im}(\Delta\omega)/[(3)^{1/2}\Gamma_0 k_0 c/2]$ versus the normalized pump strength $\Omega_B/\Gamma_0 k_0 c$ calculated from Eq.(72). It is evident from Eq.(72) and Fig. 2 that $\mathrm{Im}(\Delta\omega)$ exhibits a simple scaling with $\Omega_B/\Gamma_0 k_0 c$ only in the asymptotic limits in Eqs.(73) and (74). Moreover, the instability growth rate is greatly reduced as the pump strength is increased to large values [compare Eqs.(73) and (74)]. Although the details will not be presented here, it is also found[20] that the instability bandwidth in ΔK-space decreases substantially as $\Omega_B/\Gamma_0 k_0 c$ is increased. Indeed, the range of $\widetilde{\Delta K}$

corresponding to instability can be approximated by $|\widetilde{\Delta K}| < \Delta K_b \equiv \Gamma_0 k_0 \times (2\Gamma_0 k_0 c/\Omega_B)^{\frac{1}{2}}$ in the strong-pump regime with $\Omega_B/\Gamma_0 k_0 c >> 1$.

(d) As a final point, because $\Gamma_0 \propto \hat{n}_T^{1/3}$, the scaling of $\mathrm{Im}(\delta\omega)$ with trapped electron density $\hat{n}_T$ (or current) varies from $\hat{n}_T^{1/3}$ in the weak-pump regime [Eq.(73)] to $\hat{n}_T^{1/2}$ in the strong-pump regime [Eq.(74)]. This is in contrast with the analysis in Sec. VI where <u>all</u> of the electrons are deeply trapped and the characteristic growth rate scales as $\hat{n}_T^{1/3}$ in the strong-pump regime ($\Omega_B >> \Gamma_0 k_0 c$) and as $\hat{n}_T^{2/3}$ in the weak-pump regime ($\Omega_B << \Gamma_0 k_0 c$).

VI. SIDEBAND INSTABILITY FOR PRIMARY ELECTROMAGNETIC WAVE WITH SLOWLY VARYING PHASE

In this section, we make use of Eqs.(24), (25) and (35) to investigate detailed properties of the sideband instability in circumstances where all of the electrons are deeply trapped near the bottom of the ponderomotive potential with energy $\gamma_j' \simeq \hat{\gamma}_-'$ [Eq.(52)] and average density $\hat{n}_T' = \hat{n}_T/\gamma_p = \text{const.}$ For deeply trapped electrons, Eqs.(24), (25) and (35) can be approximated by

$$\left(\frac{\partial}{\partial t'} + \frac{c^2 k_s'}{\omega_s'}\frac{\partial}{\partial z'}\right)\hat{a}_s = \frac{a_w \hat{\omega}_{pT}^2}{2\omega_s'\hat{\gamma}'}\sin(\theta_s' + \delta_s') \ , \tag{75}$$

$$\hat{a}_s\left(\frac{\partial}{\partial t'} + \frac{c^2 k_s'}{\omega_s'}\frac{\partial}{\partial z'}\right)\delta_s' = \frac{a_w \hat{\omega}_{pT}^2}{2\omega_s'\hat{\gamma}'}\cos(\theta_s' + \delta_s') \ , \tag{76}$$

$$\frac{d^2}{dt'^2}\theta_s' + \frac{c^2 k_p'^2 a_w \hat{a}_s}{\hat{\gamma}'^2}\sin(\theta_s' + \delta_s') = 0 \ , \tag{77}$$

where $\hat{\omega}_{pT}^2 = 4\pi\hat{n}_T' e^2/m$. In Eqs.(75)-(77), the subscript j has been dropped from θ_{js}'; use has been made of $a_s = \hat{a}_s \exp(i\delta_s')$; and we have taken the characteristic energy of the trapped electrons to be $\hat{\gamma}' = (1 + a_w^2)^{\frac{1}{2}}$ [Eq.(41)]. Moreover, $\theta_s' + \delta_s' \simeq 2n\pi$ $(n = 0, \pm 1, \pm 2, \cdots)$ for the deeply trapped electrons assumed in Eqs.(75)-(77). Without loss of generality, we take $n = 0$ and expand Eqs.(75)-(77) for small $\theta_s' + \delta_s'$. This readily gives

$$\left(\frac{\partial}{\partial t'} + \frac{c^2 k_s'}{\omega_s'}\frac{\partial}{\partial z'}\right)\hat{a}_s = \frac{a_w \hat{\omega}_{pT}^2}{2\omega_s'\hat{\gamma}'}(\theta_s' + \delta_s') \ , \tag{78}$$

$$\hat{a}_s\left(\frac{\partial}{\partial t'} + \frac{c^2 k_s'}{\omega_s'}\frac{\partial}{\partial z'}\right)\delta_s' = \frac{a_w \hat{\omega}_{pT}^2}{2\omega_s'\hat{\gamma}'} \ , \tag{79}$$

$$\frac{d^2}{dt'^2}\theta_s' + \frac{c^2k_p'^2a_w\hat{a}_s}{\hat{\gamma}'^2}(\theta_s' + \delta_s') = 0 , \tag{80}$$

correct to lowest order. Unlike the analysis in Sec. V, a striking feature of Eqs.(78)-(80) is that there is necessarily a variation in the zero-order wave phase δ_s^0 predicted by Eq.(79).

A. Equilibrium Model

An appropriate quasi-steady equilibrium state consistent with Eqs.(78)-(80) is described by

$$\theta_s^0 + \delta_s^0 = 0 , \tag{81}$$

$$\frac{\partial}{\partial t'}\hat{a}_s^0 = 0 = \frac{\partial}{\partial z'}\hat{a}_s^0 , \tag{82}$$

and

$$\frac{\partial}{\partial t'}\delta_s^0 = 0 ,$$
$$\hat{a}_s^0\frac{c^2k_s'}{\omega_s'}\frac{\partial}{\partial z'}\delta_s^0 = \frac{a_w\hat{\omega}_{pT}^2}{2\omega_s'\hat{\gamma}'} . \tag{83}$$

That is, the equilibrium wave amplitude $\hat{a}_s^0$ is constant (independent of z' and t'), whereas there is a slow variation of wave phase δ_s^0 with z' described by Eq.(83). Making use of $\omega_s' = \gamma_p k_0 v_p$ and $k_p' = \gamma_p(1 + v_p/c)k_0$ [Eq.(38)], it is readily shown that

$$\frac{a_w\hat{\omega}_{pT}^2}{2\omega_s'\hat{\gamma}'\hat{a}_s^0} = 2\Gamma_0\left(\frac{\Gamma_0 ck_0}{\Omega_B}\right)^2 k_p'c , \tag{84}$$

where the small parameter $\Gamma_0^3 << 1$ is defined in Eq.(39), and $\Omega_B = (c^2k_p'^2a_w\hat{a}_s^0/\hat{\gamma}'^2\gamma_p^2)^{\frac{1}{2}}$ is the bounce frequency (in the laboratory frame) for

deeply trapped electrons. Neglecting beam dielectric effects, we approximate $\omega_s' = ck_s'$ on the left-hand side of Eq.(83), and Eq.(83) can be expressed as

$$\frac{\partial}{\partial z'} \delta_s^0 = \varepsilon k_p' , \tag{85}$$

where the small parameter ε is defined by

$$\varepsilon = 2\Gamma_0 \left(\frac{\Gamma_0 c k_0}{\Omega_B} \right)^2 << 1 . \tag{86}$$

Note that $\varepsilon << 1$ is required in the present analysis in order that the change in δ_s^0 is small over the scale length of the ponderomotive potential ($\lambda_p' = 2\pi k_p'^{-1}$). Unlike the stability analysis in Sec. V, Eq.(86) requires that the pump amplitude be above a certain small threshold value ($\Omega_B^2/c^2k_0^2 >> 2\Gamma_0^3$) for the present analysis to be valid.

B. Linear Stability Analysis and Dispersion Relation

We now express $\hat{a}_s = \hat{a}_s^0 + \delta\hat{a}_s$, $\delta_s' = \delta_s^0 + \tilde{\delta}_s'$ and $\theta_s' = \theta_s^0 + \delta\theta_s'$, where $\delta\hat{a}_s$, $\tilde{\delta}_s'$ and $\delta\theta_s'$ denote small perturbations. Linearizing Eqs.(78)-(80) about the equilibrium state described by Eqs.(81)-(83) readily gives

$$\left(\frac{\partial}{\partial t'} + \frac{c^2 k_s'}{\omega_s'} \frac{\partial}{\partial z'} \right) \delta\hat{a}_s = \varepsilon \hat{a}_s^0 c k_p' (\delta\theta_s' + \tilde{\delta}_s') , \tag{87}$$

$$\hat{a}_s^0 \left(\frac{\partial}{\partial t'} + \frac{c^2 k_s'}{\omega_s'} \frac{\partial}{\partial z'} \right) \tilde{\delta}_s' + \delta\hat{a}_s \varepsilon c k_p' = 0 , \tag{88}$$

$$\frac{d^2}{dt'^2} \delta\theta_s' + \hat{\omega}_B^2(\hat{\gamma}')(\delta\theta_s' + \tilde{\delta}_s') = 0 . \tag{89}$$

Here, $\hat{\omega}_B(\hat{\gamma}') = (c^2k_p'^2a_w\hat{a}_s^0/\hat{\gamma}'^2)^{\frac{1}{2}}$, ε is the small parameter defined in Eq.(86) [see also Eq.(84)], and use has been made of $\omega_s' = ck_s'$ and Eq.(85) to express $\delta\hat{a}_s(c^2k_s'/\omega_s')(\partial\delta_s^0/\partial z') = \delta\hat{a}_s\varepsilon ck_p'$ in Eq.(88). As in Sec. V, we assume that the z'- and t'- dependence of the perturbed quantities in Eqs.(87)-(89) is proportional to $\exp[-i(\Delta\omega')t' + i(\Delta k')z']$, where $\mathrm{Im}(\Delta\omega') > 0$ corresponds to temporal growth. Approximating $\omega_s' = ck_s'$, Eqs.(87)-(89) readily give

$$-i(\Delta\omega' - c\Delta k')\delta\hat{a}_s = \varepsilon\hat{a}_s^0 ck_p'(\delta\theta_s' + \tilde{\delta}_s') \ , \tag{90}$$

$$-i\hat{a}_s^0(\Delta\omega' - c\Delta k')\tilde{\delta}_s' = -\varepsilon ck_p'\delta\hat{a}_s \ , \tag{91}$$

$$[(\Delta\omega')^2 - \hat{\omega}_B^2(\hat{\gamma}')](\delta\theta_s' + \tilde{\delta}_s') = (\Delta\omega')^2\tilde{\delta}_s' \ . \tag{92}$$

After some straightforward algebraic manipulation, Eqs.(90)-(92) give the desired dispersion relation[70]

$$0 = 1 - \frac{\hat{\omega}_B^2(\hat{\gamma}')}{(\Delta\omega')^2} - \frac{\varepsilon^2c^2k_p'^2}{(\Delta\omega' - c\Delta k')^2} \ , \tag{93}$$

which determines $\Delta\omega'$ in terms of $\Delta k'$ and other system parameters.

Paralleling the analysis in Sec. V, we transform $\Delta\omega'$ and $\Delta k'$ back to the laboratory frame according to Eq.(65). Making use of Eqs.(65)-(67) and the relations $k_p' = \gamma_p(1 + v_p/c)k_0$ [Eq.(38)] and $\varepsilon = 2\Gamma_0(\Gamma_0ck_0/\Omega_B)^2$ [Eq.(86)], it is readily shown that Eq.(93) can be expressed in the equivalent form

$$0 = 1 - \frac{\Omega_B^2}{(\Delta\Omega)^2} - \frac{\Omega_B^2 4(\Gamma_0ck_0/\Omega_B)^6}{(\Delta\Omega - c\Delta K)^2} \ . \tag{94}$$

Here, $\Delta\Omega \equiv \Delta\omega - v_p\Delta k$, $\Delta K \equiv k_0(v_p/c)(\Delta k/k_s)$, and $\Omega_B = (c^2k_p'^2a_w\hat{a}_s^0/\gamma_p^2\hat{\gamma}'^2)^{\frac{1}{2}}$ is the bounce frequency (in the laboratory frame) for deeply trapped electrons.

C. Sideband Instability

Equation (94) has the familiar form of the dispersion relation for the two-stream instability.[71,72] Here, $\Omega_B^2 \to \hat{\omega}_{p1}^2$ plays the role of the first plasma component, and $\Omega_B^2 4(\Gamma_0 ck_0/\Omega_B)^6 \to \hat{\omega}_{p2}^2$ plays the role of the second plasma component which is drifting with velocity c relative to the first component. Equation (94) can be solved numerically for the real oscillation frequency $\mathrm{Re}(\Delta\Omega)$ and growth rate $\mathrm{Im}(\Delta\Omega)$ in terms of $c\Delta K$, Ω_B and $\Omega_B/\Gamma_0 k_0 c$ over a wide range of system parameters. For present purposes, we make use of analytical estimates to determine the instability bandwidth and maximum growth rate from Eq.(94).

First, it can be shown from Eq.(94) that instability exists [$\mathrm{Im}(\Delta\Omega) = \mathrm{Im}(\delta\omega) > 0$] for ΔK in the range

$$-\Delta K_b < \Delta K < \Delta K_b \ , \tag{95}$$

where the bandwidth ΔK_b is given (exactly) by

$$c\Delta K_b = \Omega_B \left\{ 1 + \left[4 \left(\frac{\Gamma_0 ck_0}{\Omega_B} \right)^6 \right]^{1/3} \right\}^{3/2} \ . \tag{96}$$

As illustrated schematically in Fig. 3, the growth rate $\mathrm{Im}(\Delta\Omega) = \mathrm{Im}(\delta\omega)$ is equal to zero for $\Delta K = 0$ and $\Delta K = \pm\Delta K_b$, and achieves its maximum value at $\Delta K = \pm\Delta K_M$. Equation (96) is valid for arbitrary pump strength ranging from the strong-pump regime ($\Omega_B/\Gamma_0 k_0 c \gg 1$) to the weak-pump regime ($\Omega_B/\Gamma_0 k_0 c \ll 1$). Moreover, it can be shown exactly from Eq.(94) that the real oscillation frequency of the unstable branch increases from

$$\mathrm{Re}(\Delta\Omega) = 0, \text{ for } \Delta K = 0 \ , \tag{97}$$

to

$$\mathrm{Re}(\Delta\Omega) = +\Omega_B \left\{ 1 + \left[4 \left(\frac{\Gamma_0 c k_0}{\Omega_B} \right)^6 \right]^{1/3} \right\}^{1/2} , \text{ for } \Delta K = +\Delta K_b . \qquad (98)$$

The range of oscillation frequencies described by Eqs.(97) and (98) corresponds to the upper sideband. On the other hand, for ΔK in the interval $-\Delta K_b < \Delta K < 0$, the lower sideband is unstable, and the polarity of $\mathrm{Re}(\Delta\Omega)$ is reversed relative to Eq.(98). Because $\mathrm{Im}(\Delta\Omega)$ is an even function of ΔK, and $\mathrm{Re}(\Delta\Omega)$ is an odd function of ΔK, without loss of generality we limit the subsequent analysis to the interval $0 < \Delta K < \Delta K_b$.

Although the bandwidth ΔK_b can be calculated analytically for arbitrary pump strength $\Omega_B/\Gamma_0 c k_0$ [Eq.(96)], the growth rate $\mathrm{Im}(\Delta\Omega)$ must generally be determined numerically from Eq.(94). However, analytical estimates of the maximum growth rate can be made in both the weak-pump and strong-pump limits. In this regard, it should be kept in mind that $\Gamma_0 \ll 1$ is assumed in the present analysis [Eq.(39)].

Weak-Pump Regime ($\Omega_B/\Gamma_0 c k_0 \ll 1$): In the weak-pump regime with $\Omega_B/\Gamma_0 c k_0 \ll 1$, we also require $(\Omega_B/\Gamma_0 c k_0)^2 \gg 2\Gamma_0$ in order to be consistent with the assumption of slowly varying phase δ_s^0, i.e., $\varepsilon \ll 1$ in Eq.(86). For $\Omega_B/\Gamma_0 c k_0 \ll 1$, it follows from Eq.(96) that the instability bandwidth is given approximately by

$$c\Delta K_b = 2\Gamma_0 c k_0 \left(\frac{\Gamma_0 c k_0}{\Omega_B} \right)^2 \left[1 + \frac{3}{(2)^{5/3}} \left(\frac{\Omega_B}{\Gamma_0 c k_0} \right)^2 + \cdots \right] . \qquad (99)$$

Because $(\Omega_B/\Gamma_0 c k_0)^2 \gg 2\Gamma_0$ is required, we note from Eq.(99) that the instability bandwidth ΔK_b in the weak-pump regime is relatively narrow in units of k_0. It can also be shown from Eq.(94) that the maximum growth rate $\mathrm{Im}(\Delta\Omega)_M = \mathrm{Im}(\Delta\omega)_M$ in the weak-pump regime can be approximated by

$$\mathrm{Im}(\Delta\Omega)_M = \frac{(3)^{1/2}}{2}\,\Gamma_0 ck_0 \quad . \tag{100}$$

Moreover, maximum growth occurs for $\Delta K = \Delta K_M$, where ΔK_M is defined by

$$c\Delta K_M = 2\Gamma_0 ck_0\left(\frac{\Gamma_0 ck_0}{\Omega_B}\right)^2\left[1 + \frac{3}{16}\left(\frac{\Omega_B}{\Gamma_0 ck_0}\right)^4 + \cdots\right] \quad . \tag{101}$$

Comparing Eqs.(99) and (101), we note that ΔK_M is only slightly downshifted from ΔK_b. That is, the growth rate $\mathrm{Im}(\Delta\Omega)$ is peaked very close to the upper end of the unstable wavenumber range in Fig. 3.

For specified values of $\Gamma_0 ck_0$ and $\Omega_B/\Gamma_0 ck_0 \ll 1$, it is evident from Eqs.(73) and (100) that the growth rate in Eq.(100) is the same as the corresponding growth rate derived in Sec. V in the weak-pump regime. Moreover, because $\Gamma_0 \propto \hat{n}_T^{1/3}$, the scaling of the growth rate with trapped-electron density (or current) is proportional to $\hat{n}_T^{1/3}$ in Eqs.(73) and (100).

Strong-Pump Regime ($\Omega_B/\Gamma_0 ck_0 \gg 1$): For $\Omega_B/\Gamma_0 ck_0 \gg 1$, it follows from Eq.(96) that the instability bandwidth ΔK_b is given approximately by

$$c\Delta K_b = \Gamma_0 ck_0\left(\frac{\Omega_B}{\Gamma_0 ck_0}\right)\left[1 + \frac{3}{(2)^{1/3}}\left(\frac{\Gamma_0 ck_0}{\Omega_B}\right)^2 + \cdots\right] \quad . \tag{102}$$

In units of $\Gamma_0 k_0$, it follows from Eq.(102) that the instability bandwidth ΔK_b is also relatively broad in the strong-pump regime. This is in contrast with the constant-phase case analyzed in Sec. V, where the (narrow) bandwidth ΔK_b is given approximately by $\Delta K_b = \Gamma_0 k_0 (2\Gamma_0 k_0 c/\Omega_B)^{\frac{1}{2}}$ in the strong-pump regime with $\Omega_B/\Gamma_0 k_0 c \gg 1$. Moreover, it can be shown from Eq.(94) that the maximum growth rate in the strong-pump regime can be approximated by

$$\mathrm{Im}(\Delta\Omega)_M = \frac{(3)^{1/2}}{(2)^{2/3}}\,\Gamma_0 ck_0\left(\frac{\Gamma_0 ck_0}{\Omega_B}\right) \quad . \tag{103}$$

Here, maximum growth occurs for $\Delta K = \Delta K_M$, where ΔK_M is defined by

$$c\Delta K_M = \Gamma_0 ck_0\left(\frac{\Omega_B}{\Gamma_0 ck_0}\right)\left[1 + \frac{3}{(2)^{4/3}}\left(\frac{\Gamma_0 ck_0}{\Omega_B}\right)^2 + \cdots\right] \quad . \tag{104}$$

Comparing Eqs.(74) and (103) for specified values of $\Gamma_0 ck_0$ and $\Omega_B/\Gamma_0 ck_0 >> 1$, it follows that the growth rate in Eq.(103) is smaller than the corresponding growth rate derived in Sec. V in the strong-pump regime. Moreover, because $\Gamma_0 \alpha \hat{n}_T^{1/3}$, the growth rate scaling is proportional to $\hat{n}_T^{1/2}$ in Eq.(74) and proportional to $\hat{n}_T^{2/3}$ in Eq.(103).

Intermediate Pump Strength: The dispersion relation (94) must generally be solved numerically when $\Omega_B/\Gamma_0 ck_0 \approx 1$. However, for the special case where

$$\frac{\Omega_B}{\Gamma_0 ck_0} = (2)^{1/3} \quad , \tag{105}$$

the dispersion relation (94) can be solved exactly. Substituting Eq.(105) into Eq.(94) gives

$$0 = 1 - \frac{\Omega_B^2}{(\Delta\Omega)^2} - \frac{\Omega_B^2}{(\Delta\Omega - c\Delta K)^2} \quad , \tag{106}$$

which is the two-stream dispersion relation for "equidensity" streams with effective plasma frequency Ω_B. It is readily shown from Eq.(106) that instability exists for ΔK in the range $-\Delta K_b < \Delta K < \Delta K_b$ where

$$c\Delta K_b = (2)^{3/2}\Omega_B \quad . \tag{107}$$

Moreover, the growth rate $\mathrm{Im}(\Delta\Omega)$ and real oscillation frequency $\mathrm{Re}(\Delta\Omega)$ of the unstable branch are given by

$$\mathrm{Im}(\Delta\Omega) = \Omega_B \left\{ \left[1 + 8(\Delta K/\Delta K_b)^2 \right]^{1/2} - 1 - 2(\Delta K/\Delta K_b)^2 \right\}^{1/2} \tag{108}$$

and

$$\mathrm{Re}(\Delta\Omega) = (2)^{1/2}\Omega_B(\Delta K/\Delta K_b) = c\Delta K/2 \tag{109}$$

for ΔK in the interval $-\Delta K_b < \Delta K < \Delta K_b$. The maximum growth rate calculated from Eq.(108) is

$$\mathrm{Im}(\Delta\Omega)_M = \frac{1}{2}\,\Omega_B \ , \tag{110}$$

which occurs for $\Delta K = \pm\Delta K_M$, where ΔK_M is defined by

$$\Delta K_M = \left(\frac{3}{8}\right)^{1/2} \Delta K_b \ . \tag{111}$$

At intermediate pump strengths ($\Omega_B/\Gamma_0 ck_0 \approx 1$), it is clear from Eqs.(109)-(111) that the characteristic oscillation frequency and growth rate of the sideband instability are of order the bounce frequency Ω_B.

Comparing Eqs.(100) and (110) for specified $\Gamma_0 k_0 c$, it is evident that the maximum growth rate $\mathrm{Im}(\Delta\Omega)_M$ varies only slightly for $\Omega_B/\Gamma_0 ck_0$ in the range $2\Gamma_0 < \Omega_B/\Gamma_0 ck_0 \leq (2)^{1/3}$. On the other hand, in the strong-pump regime with $\Omega_B/\Gamma_0 ck_0 >> 1$, it follows from Eq.(103) that $\mathrm{Im}(\Delta\Omega)_M$ decreases rapidly with $\mathrm{Im}(\Delta\Omega)_M = \left[(3)^{1/2}/(2)^{2/3}\right]\Gamma_0 ck_0(\Gamma_0 ck_0/\Omega_B)$. This is illustrated in Fig. 4 where the normalized maximum growth rate $\mathrm{Im}(\Delta\Omega)_M/\left[(3)^{1/2}\Gamma_0 ck_0/2\right]$ calculated numerically from the dispersion relation (94) is plotted versus the dimensionless pump strength $\Omega_B/\Gamma_0 ck_0$.

Finally, Table 1 provides a concise summary which compares the key stability results obtained from the dispersion relation (68) ($\delta_s^0 = \text{const.}$) and the dispersion relation (94) ($\partial\delta_s^0/\partial z' = \varepsilon k_p' \neq 0$). In particular, presented in Table 1 are the normalized maximum growth rate $\mathrm{Im}(\Delta\Omega)_M/\Gamma_0 ck_0$, the normalized

instability bandwidth $\Delta K_b/\Gamma_0 k_0$, and the normalized real oscillation frequency at maximum growth $\mathrm{Re}(\Delta\Omega)_M/\Gamma_0 ck_0$, for pump strengths ranging from the weak-pump regime ($\Omega_B/\Gamma_0 ck_0 << 1$) to the strong-pump regime ($\Omega_B/\Gamma_0 ck_0 >> 1$). For $\Omega_B/\Gamma_0 ck_0 >> 1$, a very striking result evident from Table 1 is that the sideband instability described by Eq.(94) has a broad bandwidth with $\Delta K_b/\Gamma_0 k_0 = \Omega_B/\Gamma_0 ck_0 >> 1$, whereas the sideband instability described by Eq.(68) has a narrow bandwidth with $\Delta K_b/\Gamma_0 k_0 = (2\Gamma_0 ck_0/\Omega_B)^{\frac{1}{2}} << 1$.

It should also be pointed out that the frequency bandwidth $\Delta\omega_b$ can be estimated in the various regimes illustrated in Table 1. For example, in the case of slowly varying equilibrium phase [Eq.(94)], we obtain $\Delta\Omega_b = \Delta\omega_b - v_p\Delta k_b \simeq \pm\Omega_B$ in the strong-pump regime ($\Omega_B/\Gamma_0 ck_0 >> 1$). Here, $v_p\Delta k_b = c(k_s/k_0)\Delta K_b = \gamma_p^2(1 + v_p/c)(v_p/c)\Omega_B$ follows from Eqs.(37), (67) and (102). This gives $\Delta\omega_b \simeq \gamma_p^2(1 + v_p/c)(v_p/c)\Omega_B \pm \Omega_B$, where the term $\pm\Omega_B$ represents a small correction.

VII. CONCLUSIONS

In the present analysis, a single-particle model based on Eqs.(24), (25) and (35) has been used to investigate properties of the sideband instability for small-amplitude perturbations about a primary electromagnetic wave with constant amplitude $\hat{a}_s^0$ = const. (independent of z' and t'). Two cases were treated. The first case (Sec. V) assumed constant equilibrium wave phase δ_s^0 = const., which requires (for self-consistency) both untrapped- and trapped-electron populations satisfying $\langle \sum_j \gamma_j'^{-1} \exp(i\theta_{js}^0 + i\delta_s^0) \rangle = 0$ [Eq.(49)]. This is analogous to the case studied by Davidson et. al.[19-21] using the Vlasov-Maxwell equations. The second case (Sec. VI) assumed that all of the electrons are trapped, which requires a slow spatial variation of the equilibrium wave phase $\partial\delta_s^0/\partial z' \neq 0$.[32-42] The resulting dispersion relations and detailed stability properties were found to be quite different in the two cases. For deeply trapped electrons, it was shown that the dispersion relations are given by Eq.(68) for δ_s^0 = const., and by Eq.(94) for $\partial\delta_s^0/\partial z' = 2\Gamma_0(\Gamma_0 ck_0/\Omega_B)^2 k_p' \neq 0$. The two dispersion relations and the corresponding properties of the sideband instability were examined in detail in Secs. V and VI. We summarize below some of the key results.

First, in the weak-pump regime ($\Omega_B/\Gamma_0 ck_0 \ll 1$), the characteristic maximum growth rate of the sideband instability is substantial, with $\mathrm{Im}(\Delta\Omega)_M/\Gamma_0 ck_0 = (3)^{1/2}/2$ in both cases [Eqs.(73) and (100)]. Second, in the strong-pump regime ($\Omega_B/\Gamma_0 ck_0 \gg 1$), it is found that the maximum growth rate is reduced significantly, with $\mathrm{Im}(\Delta\Omega)_M/\Gamma_0 ck_0 = 2^{-1/2}(\Gamma_0 ck_0/\Omega_B)^{1/2} \ll 1$ for the case of constant phase δ_s^0 [Eq.(68)], and $\mathrm{Im}(\Delta\Omega)_M/\Gamma_0 ck_0 = \left[(3)^{1/2}/(2)^{2/3}\right](\Gamma_0 ck_0/\Omega_B) \ll 1$ for the case of slowly varying δ_s^0 [Eq.(94)]. It is also found that the instability bandwidth ΔK_b in ΔK-space is generally

different in the two cases. For example, in the strong-pump regime ($\Omega_B/\Gamma_0 ck_0 >> 1$), we obtain $\Delta K_b/\Gamma_0 k_0 = (2\Gamma_0 ck_0/\Omega_B)^{1/2} << 1$ from Eq.(68), whereas $\Delta K_b/\Gamma_0 k_0 = \Omega_B/\Gamma_0 ck_0 >> 1$ follows from Eq.(94). Finally, for the case of slowly varying phase δ_s^0 [Eq.(94)], it is found that both the upper and lower sidebands are unstable, with $Re(\Delta\Omega) > 0$ for $\Delta K > 0$ and $Re(\Delta\Omega) < 0$ for $\Delta K < 0$. In contrast, for $\delta_s^0 = const.$, it is found from Eq.(68) that only the lower sideband is unstable. This is associated with the fact that the wave perturbation is assumed to have right-circular polarization in deriving Eq.(68).[19] For $\delta_s^0 = const.$ and wave perturbations with left-circular polarization, it is readily shown that the upper sideband is unstable.[19]

ACKNOWLEDGMENTS

This research was supported in part by the Los Alamos National Laboratory and in part by the Office of Naval Research. It is a pleasure to acknowledge the benefit of useful discussions with Richard Aamodt, Marshall Rosenbluth, Andrew Sessler, and Simon Yu.

VIII. REFERENCES

1. C.A. Brau, IEEE J. Quantum Electronics QE-21, 824 (1985).
2. R.W. Warren, B.E. Newmam and J.C. Goldstein, IEEE J. Quantum Electronics QE-21, 882 (1985).
3. T.J. Orzechowski, B. Anderson, W.M. Fawley, D. Prosnitz, E.T. Scharlemann, S. Yarema, D.B. Hopkins, A.C. Paul, A.M. Sessler and J.S. Wurtele, Phys. Rev. Lett. 54, 889 (1985).
4. T.J. Orzechowski, E.T. Scharlemann, B. Anderson, V.K. Neil, W.M. Fawley, D. Prosnitz, S.M. Yarema, D.B. Hopkins, A.C. Paul, A.M. Sessler and J.S. Wurtele, IEEE J. Quantum Electronics QE-21, 831 (1985).
5. M. Billardon, P. Elleaume, J.M. Ortega, C. Bazin, M. Bergher, M. Velghe, D.A.G. Deacon, and Y. Petroff, IEEE J. Quantum Electronics, QE-21, 805 (1985).
6. J. Masud, T.C. Marshall, S.P. Schlesinger, and F.G. Yee, Phys. Rev. Lett. 56, 1567 (1986).
7. J. Fajans, G. Bekefi, Y.Z. Yin and B. Lax, Phys. Rev. Lett. 53, 246 (1984).
8. R.W. Warren, B.E. Newmam, J.G. Winston, W.E. Stein, L.M. Young and C.A. Brau, IEEE J. Quantum Electronics QE-19, 391 (1983).
9. G. Bekefi, R.E. Shefer and W.W. Destler, Appl. Phys. Lett. 44, 280 (1983).
10. C.W. Roberson, J.A. Pasour, F. Mako, R.F. Lucey, Jr., and P. Sprangle, Infrared and Millimeter Waves 10, 361 (1983), and references therein.
11. A. Grossman, T.C. Marshall, and S.P. Schlesinger, Phys. Fluids 26, 337 (1983).
12. D. Prosnitz and A.M. Sessler, in Physics of Quantum Electronics (Addison-Wesley, Reading, Mass.) 9, 651 (1982).

13. R.K. Parker, R.H. Jackson, S.H. Gold, H.P. Freund, V.L. Granatstein, P.C. Efthimion, M. Herndon, and A.K. Kinkead, Phys. Rev. Lett. 48, 238 (1982).

14. S. Benson, D.A.G. Deacon, J.N. Eckstein, J.M.J. Madey, K. Robinson, T.I. Smith, and R. Taber, Phys. Rev. Lett. 48A, 235 (1982).

15. A.N. Didenko, A.R. Borisov, G.R. Fomenko, A.V. Kosevnikov, G.V. Melnikov, Yu G. Stein, and A.G. Zerlitsin, IEEE Trans. Nucl. Sci. NS-28, 3169 (1981).

16. D.B. McDermott, T.C. Marshall, S.P. Schlesinger, R.K. Parker, and V.L. Granatstein, Phys. Rev. Lett. 41, 1368 (1978).

17. D.A.G. Deacon, L.R. Elias, J.M.J. Madey, G.J. Ramian, H.A. Schwettman, and T.I. Smith, Phys. Rev. Lett. 38, 892 (1977).

18. L.R. Elias, W.M. Fairbank, J.M.J. Madey, H.A. Schwettman, and T.I. Smith, Phys. Rev. Lett. 36, 717 (1976).

19. R.C. Davidson, Phys. Fluids 29, in press (1986).

20. R.C. Davidson, J.S. Wurtele and R.E. Aamodt, "Kinetic Analysis of the Sideband Instability in a Helical Wiggler Free ELectron Laser for Electrons Trapped Near the Bottom of the Ponderomotive Potential," submitted for publication (1986).

21. B. Lane and R.C. Davidson, Phys. Rev. A27, 2008 (1983).

22. A.M. Dimos and R.C. Davidson, Phys. Fluids 28, 677 (1985).

23. R.C. Davidson and Y.Z. Yin, Phys. Fluids 28, 2524 (1985).

24. T. Taguchi, K. Mima, and T. Mochizuki, Phys. Rev. Lett. 46, 824 (1981).

25. F.A. Hopf, P Meystre, M.O. Scully, and W.H. Louisell, Phys. Rev. Lett. 37, 1342 (1976).

26. R.C. Davidson and W.A. McMullin, Phys. Rev. A26, 410 (1982).

27. N.S. Ginzburg and M.A. Shapiro, Opt. Comm. 40, 215 (1982).

28. J.C. Goldstein and W.B. Colson, Proc. International Conference on Lasers (New Orleans, 1982), p. 218.

29. W.B. Colson, IEEE J. Quantum Electronics QE-17, 1417 (1981).

30. P. Sprangle, C.M. Tang, and W.M. Manheimer, Phys. Rev. A21, 302 (1980).

31. W.H. Louisell, J.F. Lam, D.A. Copeland, and W.B. Colson, Phys. Rev. A19, 288 (1979).

32. N.M. Kroll, P.L. Morton and M.N. Rosenbluth, IEEE J. Quantum Electronics QE-17, 1436 (1981).

33. D.C. Quimby, J.M. Slater and J.P. Wilcoxon, IEEE J. Quantum Electronics QE-21, 979 (1985).

34. N.S. Ginzburg and M.I. Petelin, Int. J. Electronics 59, 291 (1985).

35. C.M. Tang and P. Sprangle, Free Electron Generators of Coherent Radiation (S.F. Jacobs and M.O. Scully, eds.) SPIE 453, 11 (1983).

36. R.A. Freedman and W.B. Colson, Opt. Comm. 52, 409 (1985).

37. W.B. Colson, to be published in Proc. Seventh Int. Conf. on Free Electron Lasers (Tahoe City, California) (1985).

38. M.N. Rosenbluth, H.V. Wong and B.N. Moore, Free Electron Generators of Coherent Radiation (S.F. Jacobs and M.O. Scully, eds.) SPIE 453, 25 (1983).

39. A.T. Lin, Physics of Quantum Electronics 9, 867 (1982).

40. H. Al-Abawi, J.K. McIver, G.T. Moore and M.O. Scully, Physics of Quantum Electronics 8, 415 (1982).

41. W.B. Colson, Physics of Quantum Electronics 8, 457 (1982).

42. J. Goldstein, Free Electron Generators of Coherent Radiation (S.F. Jacobs and M.O. Scully, eds.) SPIE 453, 2 (1983).

43. R.C. Davidson and Y.Z. Yin, Phys. Rev. A30, 3078 (1984).

44. G.L. Johnston and R.C. Davidson, J. Appl. Phys. 55, 1285 (1984).

45. H.P. Freund and A.K. Ganguly, Phys. Rev. A28, 3438 (1983).

46. H.S. Uhm and R.C. Davidson, Phys. Fluids 26, 288 (1983).

47. R.C. Davidson and H.S. Uhm, J. Appl. Phys. 53, 2910 (1982).

48. H.S. Uhm and R.C. Davidson, Phys. Fluids 24, 2348 (1981).

49. R.C. Davidson, W.A. McMullin and K. Tsang, Phys. Fluids 27, 233 (1983).

50. R.C. Davidson and W.A. McMullin, Phys. Fluids 26, 840 (1983).

51. W.A. McMullin and G. Bekefi, Phys. Rev. A25, 1826 (1982).

52. R.C. Davidson and W.A. McMullin, Phys. Rev. A26, 1997 (1982).

53. W.A. McMullin and G. Bekefi, Appl. Phys. Lett. 39, 845 (1981).

54. R.C. Davidson, Phys. Fluids 29, 267 (1986).

55. R.C. Davidson and J.S. Wurtele, IEEE Trans. Plasma Science PS-13, 464 (1985).

56. H.P. Freund, R.A. Kehs and V.L. Granatstein, IEEE J. Quantum Electronics QE-21, 1080 (1985).

57. H.P. Freund and A.K. Ganguly, IEEE J. Quantum Electronics QE-21, 1073 (1985).

58. B. Hafizi and R.E. Aamodt, Phys. Rev. A29, 2656 (1984).

59. P. Sprangle, C.M. Tang and I. Bernstein, Phys. Rev. A28, 2300 (1983).

60. H.P. Freund and P. Sprangle, Phys. Rev. A28, 1835 (1983).

61. R.C. Davidson and H.S. Uhm, Phys. Fluids 23, 2076 (1980).

62. P. Sprangle and R.A. Smith, Phys. Rev. A21, 293 (1980).

63. I.B. Bernstein and J.L. Hirshfield, Physica (Utrecht) 20A, 1661 (1979).

64. T. Kwan and J.M. Dawson, Phys. Fluids 22, 1089 (1979).

65. T. Kwan, J.M. Dawson and A.T. Lin, Phys. Fluids 20, 581 (1977).

66. N.M. Kroll and W.A. McMullin, Phys. Rev. A17, 300 (1978).

67. A. Hasegawa, Bell Syst. Tech. J. 57, 3069 (1978).

68. W.B. Colson, Phys. Lett. 59A, 187 (1976).

69. V.P. Sukhatme and P.A. Wolff, J. Appl. Phys. 44, 2331 (1973).

70. M.N. Rosenbluth, private communication (1986).

71. I.B. Bernstein and S.K. Trehan, Nucl. Fus. 1, 3 (1960); cf., pp. 21-23.

72. Handbook of Plasma Physics, Volume 1 (A.A. Galeev and R.N. Sudan, eds., North Holland Publishing Co., New York, 1983) pp. 521-585; cf., pp. 546 and 547.

FIGURE CAPTIONS

Fig. 1. In the ponderomotive frame, electron motion in the phase space (z', p_z') occurs on surfaces with γ' = const.

Fig. 2. Plot of normalized growth rate $\mathrm{Im}(\Delta\omega) / \left[(3)^{1/2}\Gamma_0 ck_0/2\right]$ versus dimensionless pump strength $\Omega_B/\Gamma_0 ck_0$ for $\Delta\tilde{K} = 0$ [Eq.(72)].

Fig. 3. Schematic plot of growth rate $\mathrm{Im}(\Delta\Omega)$ versus ΔK obtained from Eq.(94).

Fig. 4. Plot of normalized maximum growth rate $\mathrm{Im}(\Delta\Omega)_M / \left[(3)^{1/2}\Gamma_0 ck_0/2\right]$ versus dimensionless pump strength $\Omega_B/\Gamma_0 ck_0$ calculated numerically from Eq.(94).

Table 1. Table showing the maximum growth rate, bandwidth, and real oscillation frequency (at maximum growth) of the sideband instability obtained from Eqs.(68) and (94) in the weak-pump ($\Omega_B/\Gamma_0 ck_0 \ll 1$), intermediate-pump ($\Omega_B/\Gamma_0 ck_0 = 1$), and strong-pump ($\Omega_B/\Gamma_0 ck_0 \gg 1$) regimes. For $\Omega_B/\Gamma_0 ck_0 = 1$, the estimates are obtained numerically from Eqs.(68) and (94).

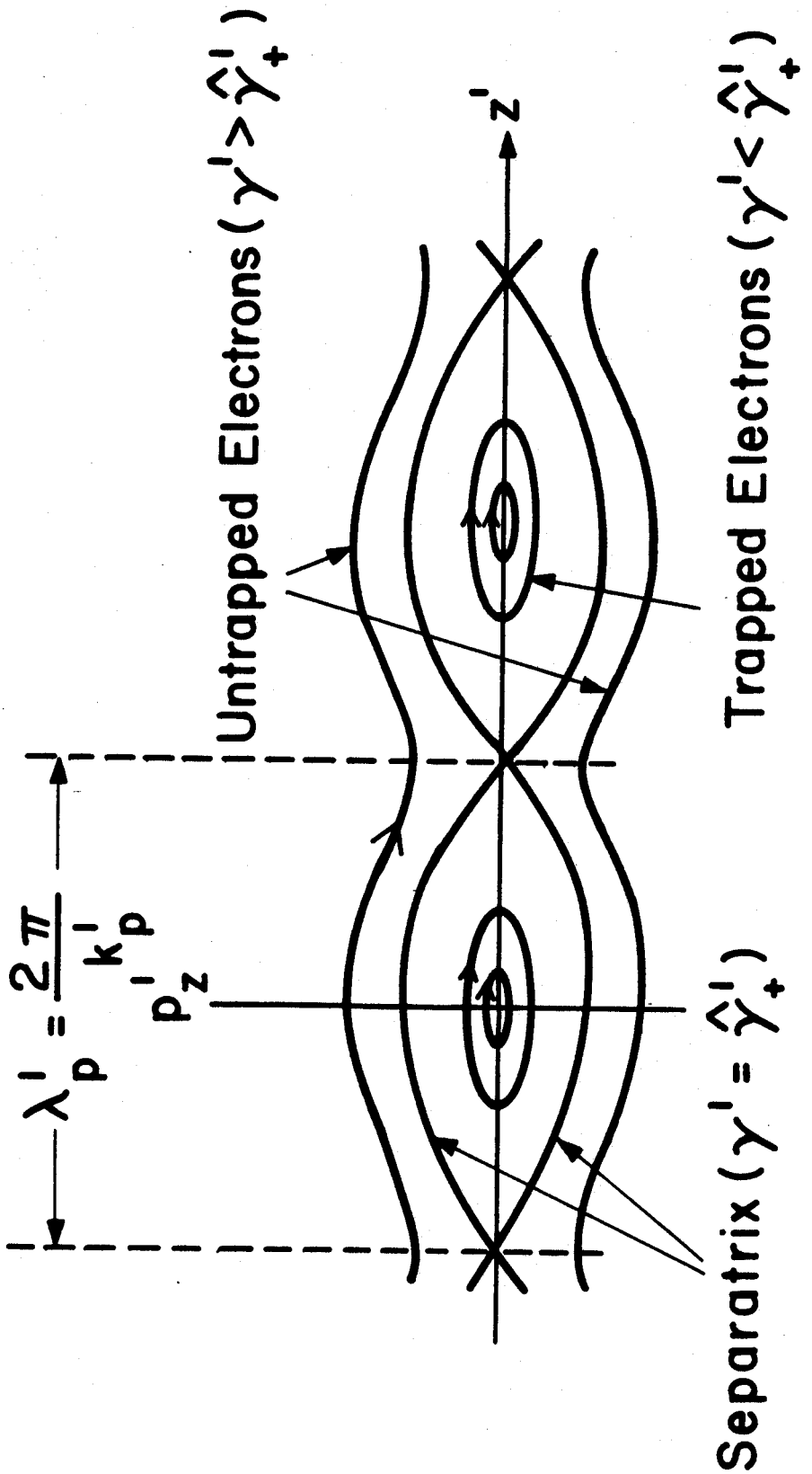
Untrapped Electrons ($\gamma' > \hat{\gamma}'_+$)
Trapped Electrons ($\gamma' < \hat{\gamma}'_+$)
Separatrix ($\gamma' = \hat{\gamma}'_+$)
z'
p'_z
$\lambda'_p = \frac{2\pi}{k'_p}$

Fig. 1

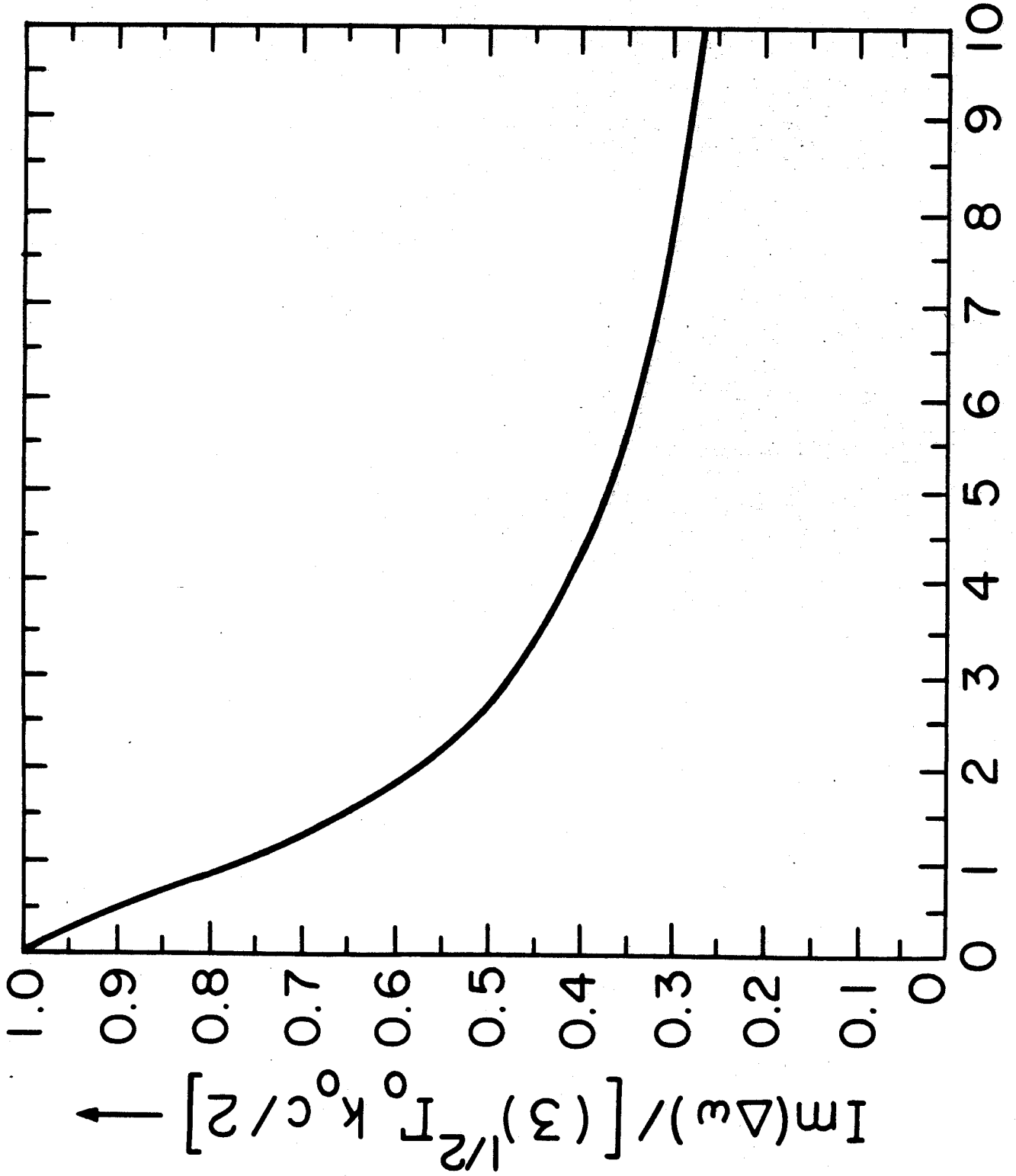
Im(Δω)/[(3)^{1/2}Γ_o k_o c/2] ⟶
0
0.1
0.2
0.3
0.4
0.5
0.6
0.7
0.8
0.9
1.0
Ω_B/Γ_o k_o c ⟶
0
1
2
3
4
5
6
7
8
9
10

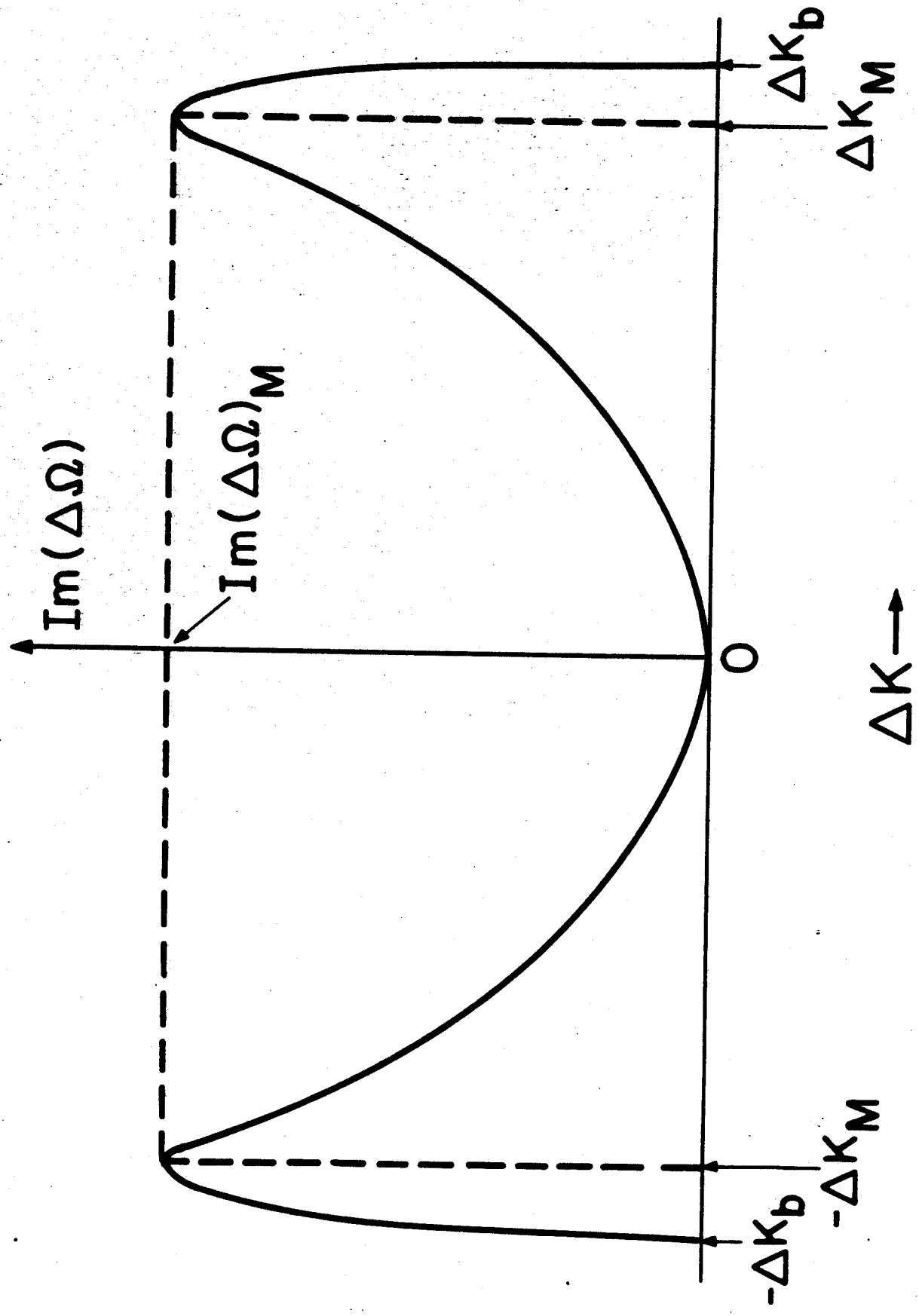

Fig. 3

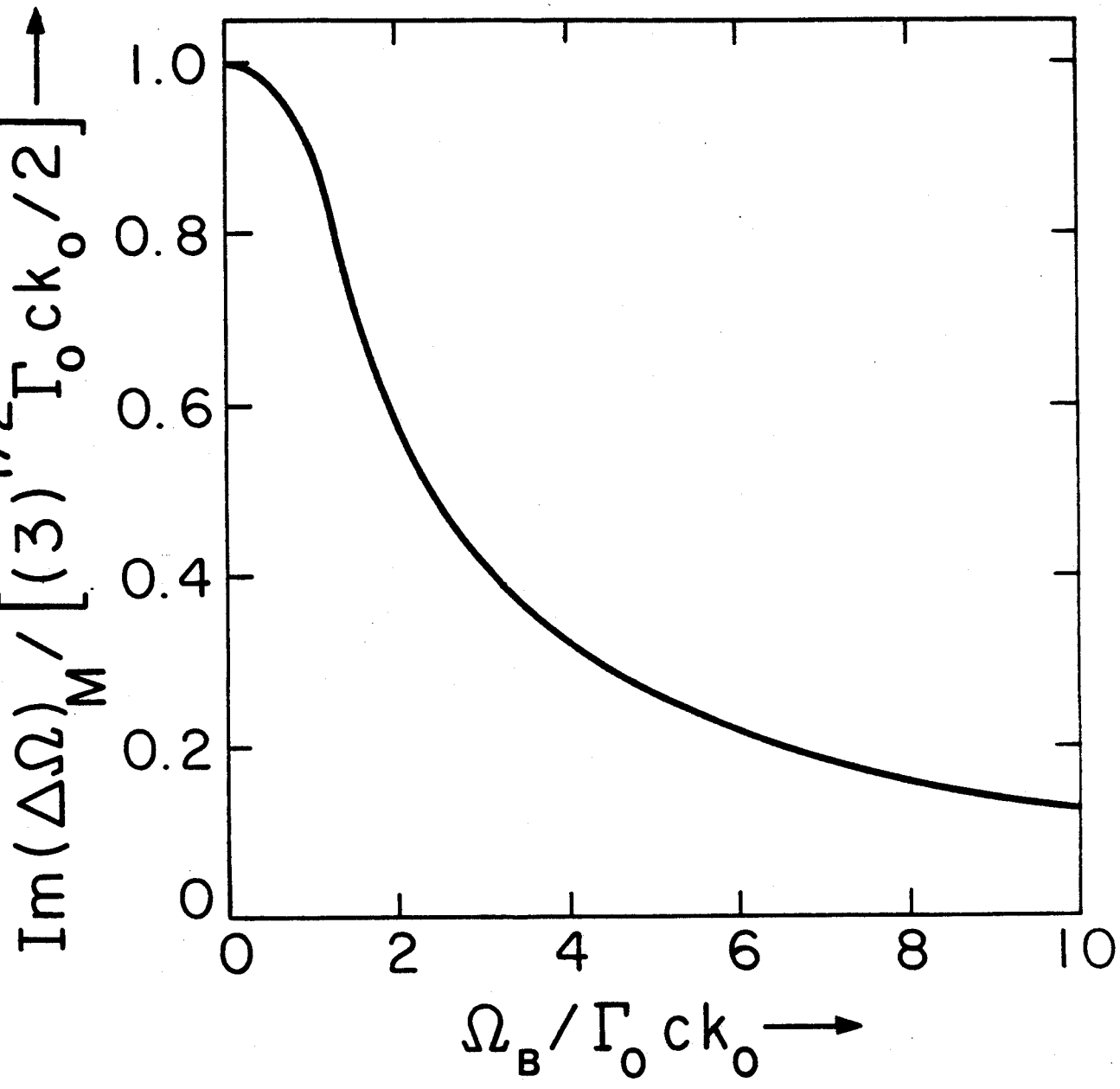
$\mathrm{Im}(\Delta\Omega)_M / [(3)^{1/2}\Gamma_o ck_o/2] \longrightarrow$
1.0
0.8
0.6
0.4
0.2
0
0
2
4
6
8
10
$\Omega_B / \Gamma_o ck_o \longrightarrow$

Fig. 4

	Dispersion Relation (68) (δ_s^0 = const.)	Dispersion Relation (94) ($\partial\delta_s^0/\partial z' = \varepsilon k_p' \neq 0$)
Weak-Pump Regime ($\Omega_B/\Gamma_0 ck_0 \ll 1$)		
$\frac{\mathrm{Im}(\Delta\Omega)_M}{\Gamma_0 ck_0}$	$\frac{(3)^{1/2}}{2}$	$\frac{(3)^{1/2}}{2}$
$\frac{\Delta K_b}{\Gamma_0 k_0}$	$\gg 1$	$2(\Gamma_0 ck_0/\Omega_B)^2$ (assumed $\ll \Gamma_0^{-1}$)
$\frac{\mathrm{Re}(\Delta\Omega)_M}{\Gamma_0 ck_0}$	$\frac{1}{2}$	$\pm\frac{1}{2}$
Intermediate-Pump Regime ($\Omega_B/\Gamma_0 ck_0 = 1$)		
$\frac{\mathrm{Im}(\Delta\Omega)_M}{\Gamma_0 ck_0}$	0.67	0.7
$\frac{\Delta K_b}{\Gamma_0 k_0}$	4	2.7
$\frac{\mathrm{Re}(\Delta\Omega)_M}{\Gamma_0 ck_0}$	-1	$\pm$ 0.9
Strong-Pump Regime ($\Omega_B/\Gamma_0 ck_0 \gg 1$)		
$\frac{\mathrm{Im}(\Delta\Omega)_M}{\Gamma_0 ck_0}$	$\left(\frac{\Gamma_0 ck_0}{2\Omega_B}\right)^{1/2}$	$\frac{(3)^{1/2}}{(2)^{2/3}}\left(\frac{\Gamma_0 ck_0}{\Omega_B}\right)$
$\frac{\Delta K_b}{\Gamma_0 k_0}$	$\left(\frac{2\Gamma_0 ck_0}{\Omega_B}\right)^{1/2}$	$\left(\frac{\Omega_B}{\Gamma_0 ck_0}\right)$
$\frac{\mathrm{Re}(\Delta\Omega)_M}{\Gamma_0 ck_0}$	$-\left(\frac{\Omega_B}{\Gamma_0 ck_0}\right)$	$\pm\left(\frac{\Omega_B}{\Gamma_0 ck_0}\right)$

Table 1